

MUTATIONS IN THE *CATB* OPERATOR-PROMOTER REGION ALLOW ALTERNATIVE  
REGULATION OF THE *BENA* PROMOTER IN *ACINETOBACTER BAYLYI* STRAIN ADP1

by

CATHERINE AILEEN PENNINGTON

(Under the Direction of Ellen Neidle)

ABSTRACT

LysR-type transcriptional regulators, BenM and CatM, tightly regulate the genes involved in aromatic compound degradation in *Acinetobacter baylyi* strain ADP1. BenM and CatM share similarities in protein sequence and promoter recognition, yet have striking differences in regulatory function. The experiments described here explore the regulatory role of CatM in the absence of a functional BenM. Spontaneous mutations in the *catB* promoter were identified in strains that maintained the ability to grow on benzoate as a sole carbon source in the absence of BenM. Characterization of the metabolism, gene expression, enzyme activity, and binding affinity of these mutants ultimately lead to a model of CatM-mediated expression of the *benA* promoter in response to increased intracellular concentrations of muconate.

INDEX WORDS: LysR-type transcriptional regulator, aromatic compound, promoter specificity, fluorescence anisotropy

MUTATIONS IN THE *CATB* OPERATOR-PROMOTER REGION ALLOW ALTERNATIVE  
REGULATION OF THE *BENA* PROMOTER IN *ACINETOBACTER BAYLYI* STRAIN ADP1

by

CATHERINE AILEEN PENNINGTON

B.S., The University of Georgia, 2003

A Thesis Submitted to the Graduate Faculty of The University of Georgia in Partial Fulfillment  
of the Requirements for the Degree

MASTER OF SCIENCE

ATHENS, GA

2009

© 2009

CATHERINE AILEEN PENNINGTON

All Rights Reserved

MUTATIONS IN THE *CATB* OPERATOR-PROMOTER REGION ALLOW ALTERNATIVE  
REGULATION OF THE *BENA* PROMOTER IN *ACINETOBACTER BAYLYI* STRAIN ADP1

by

CATHERINE AILEEN PENNINGTON

Major Professor: Ellen Neidle

Committee: Anna Karls  
Cory Momany

Electronic Version Approved:

Maureen Grasso  
Dean of the Graduate School  
The University of Georgia  
May 2009

## TABLE OF CONTENTS

	Page
LIST OF TABLES.....	vi
LIST OF FIGURES.....	vii
LIST OF ABBREVIATIONS.....	ix
CHAPTER	
1 INTRODUCTION.....	1
Purpose and Significance of this Study.....	1
Aromatic Compound Degradation.....	1
Genetic Organization & Regulation.....	2
Genetic System of <i>Acinetobacter baylyi</i> strain ADP1.....	3
LysR Type Transcriptional Regulators (LTTRs).....	4
LTTRs & RNA Polymerase.....	5
LTTR Consensus Sequence Recognition & DNA-protein Interactions.....	7
Regulation of <i>benA</i> in the Absence of BenM.....	10
Summary of Studies for this Project.....	12
2 CHARACTERIZATION OF <i>catB</i> OPERATOR-PROMOTER MUTANTS.....	19
Introduction.....	20
Materials and Methods.....	23
Results.....	28
Discussion.....	34

3	CONCLUSIONS AND FUTURE DIRECTIONS.....	56
	Conclusions.....	56
	Future Directions.....	57
	REFERENCES.....	58

## LIST OF TABLES

	Page
Table 2.1: Bacterial Strains and Plasmids.....	51
Table 2.2: Sequences of <i>catB</i> promoters used during fluorescence polarization studies .....	53
Table 2.3: Summary of CatA and Cat B enzyme activity and generation times on anthranilate and succinate .....	54
Table 2.4: Protein-DNA dissociation constants determined by fluorescence anisotropy.....	55

## LIST OF FIGURES

	Page
Figure 1.1: The $\beta$ -ketoacid pathway in <i>A. baylyi</i> ADP1.....	14
Figure 1.2: Common aromatic compounds dissimilated by microorganisms via the intermediate catechol and the $\beta$ -ketoacid pathway.....	15
Figure 1.3: Regulation of the <i>ben</i> and <i>cat</i> regions by BenM and CatM.....	16
Figure 1.4: Regulatory model of the <i>benA</i> promoter.....	17
Figure 1.5: Proposed model of CatM-activated expression of <i>benA</i> in response to increased intracellular concentration of muconate.....	18
Figure 2.1: Regulation of the <i>ben</i> and <i>cat</i> operons in wild-type cells.....	37
Figure 2.2: Model of CatM-mediated expression of the <i>ben</i> genes.....	38
Figure 2.3: Location of <i>catB</i> promoter mutations.....	39
Figure 2.4: Growth rate and metabolite concentration of wild-type and <i>catB</i> mutants.....	40
Figure 2.5: Specific activity of CatA and CatB.....	41
Figure 2.6: Ratio of CatA to CatB activity.....	42
Figure 2.7: <i>benA</i> expression in <i>catB</i> promoter mutants.....	43
Figure 2.8: EMSA of wild-type <i>catB</i> promoter and a <i>catB</i> promoter with an extra T in site one.....	44
Figure 2.9: Fluorescence Polarization Experiments.....	45
Figure 2.10: Affinity of CatM for the wild-type <i>catB</i> promoter.....	46
Figure 2.11: Affinity of CatM for the <i>catB</i> promoter containing an extra T in the site 1 spacer.....	47
Figure 2.12: Affinity of CatM for the <i>catB</i> promoter containing a point mutation at -46.....	48

Figure 2.13: Affinity of CatM for the *catB* promoter containing a point mutation at -49.....49

Figure 2.14: Proposed model of CatM-mediated expression of the *benABCDE* operon.....50

## LIST OF ABBREVIATIONS

ANT	anthranilate
BEN	benzoate
BME	beta-mercaptoethanol
CAT	catechol
DTT	dithiothreitol
EDTA	ethylenediaminetetraacetic acid
FP	fluorescence polarization
HPLC	high performance liquid chromatography
HTH	helix-turn-helix
$K_d$	dissociation constant
LTTR	LysR-type transcriptional regulator
MM	minimal medium
MUC	muconate
TCA	tricarboxylic acid
wHTH	winged helix-turn-helix

## CHAPTER I: INTRODUCTION

### **Purpose and Significance of this Study**

The purpose of this study was to characterize the protein-DNA interactions that govern the expression of genes involved in aromatic compound degradation in *Acinetobacter baylyi* strain ADP1. Aromatic compounds are prevalent in nature, often resulting from the breakdown of lignin, an aromatic polymer that may account for as much as 25% of the earth's land biomass (Harwood and Parales, 1996). These compounds may also arise from the combustion of organic material, either naturally or during human utilization of fossil fuels. Industrial and agricultural processes provide an additional source of aromatic compounds, including toxic pollutants (Dagley, 1986). The abundance and toxicity of some of these compounds is significant as they impact carbon cycling and environmental detoxification. The microbial degradation of these compounds is of particular interest because understanding and potentially harnessing the organisms involved may afford more efficient and cost effective clean up measures. Increasing the knowledge of these microorganisms, particularly with respect to metabolic regulation, may also lead to construction of biosensing organisms capable of detecting these and other hazardous compounds.

### **Aromatic Compound Degradation**

Because of its random and complex aromatic composition, lignin is difficult to degrade. However, degradation can be accomplished by a consortium of soil microorganisms (Dagley 1978). Lignin is initially degraded by extracellular enzymes secreted by fungi. The resulting simpler aromatic subunits can then be degraded by bacteria. *Acinetobacter baylyi* strain ADP1,

an aerobic, mesophilic, soil-borne, Gram-type negative, coccobacillus,  $\gamma$ -proteobacterium is an organism with this capability (Towner et al., 1991; Juni 1978; Olsen et al., 1994; Rainey et al., 1994).

In *A. baylyi*, aromatic compounds are degraded via the  $\beta$ -keto adipate pathway (Fig 1.1). As a common metabolic pathway among soil microorganisms, this pathway has been well characterized with respect to the genes, enzymes, and metabolic intermediates (Harwood and Parales, 1996). Diverse aromatic compounds are first converted to a dihydroxylated intermediate, either catechol or protocatechuate, for which the two branches of the pathway are named (Fewson, 1991). Next, specific dioxygenases catalyze *ortho*-ring cleavage, ultimately generating the tricarboxylic acid (TCA) cycle intermediates succinate and acetyl CoA. *A. baylyi* is capable of utilizing a variety of aromatic compounds as a sole source of carbon and energy. Compounds such as vanillate, shikimate, quinate, and *p*-hydroxybenzoate are metabolized through the protocatechuate branch of the  $\beta$ -keto adipate pathway, while others including benzoate (ben), salicylate, anthranilate (ant), and benzyl acetate are degraded through the catechol (cat) branch (Fig 1.2) (Bundy et al., 1998; Harwood and Parales, 1996; Jones et al., 1999; Jones et al., 2000; Segura et al., 1999).

### **Genetic Organization & Regulation**

In *A. baylyi*, the majority of genes involved in aromatic compound degradation are located in supraoperonic clusters on the chromosome (Barbe et al., 2004). Organization of these genes likely results from both the need to channel compounds through the different branches of the pathway and to ensure complete degradation of the toxic intermediates, catechol and protocatechuate (Harwood and Parales, 1996). This clustering may also allow overlapping regulation of related genes. Additionally, the proximity of related genes or genes of overlapping

function may benefit the organism by providing a means of gene regulation by duplication (Reams and Neidle, 2004).

The enzymes required for benzoate degradation are encoded by the *ben* genes (*benABCDE*) and the *cat* genes (*catA* and *catBCIJFD*) (Harwood and Parales, 1996; Neidle and Ornston, 1986; Neidle et al., 1988). Additional genes required for importing benzoate (*benPK*) are located adjacently (Clark et al., 2002; Collier et al., 1997). The expression of all genes involved is tightly regulated by two LysR-type transcriptional regulators, BenM and CatM (Bundy, 2001; Clark et al., 2002; Romero-Arroyo et al., 1995). Although BenM and CatM are 59% identical and 75% similar in protein sequence, their regulatory properties are quite different. In the presence of two effectors, benzoate and muconate, BenM activates transcription synergistically at the *benA* promoter, while CatM activates transcription of the *catB* promoter in response only to muconate (Bundy et al., 2002; Romero-Aroyo et al., 1995). Furthermore, the recognition sequences at *benA* and *catB* share some similarity, but BenM and CatM do not activate equally at the different promoters. BenM cannot regulate the *catB* promoter sufficiently to compensate for the loss of CatM, and CatM can activate the *benA* promoter, but its effect is so reduced that it cannot replace BenM (Ezezika et al., 2006). In contrast, either CatM or BenM is sufficient to activate transcription at *benP* and *catA* (Clark et al., 2002) (Fig 1.3).

### **Genetic System of *Acinetobacter baylyi* strain ADP1**

*Acinetobacter baylyi* strain ADP1 is an ideal organism for physiological and biochemical studies because of its extraordinary competence for DNA uptake. When sufficient homology exists between donor DNA and recipient *A. baylyi* DNA, natural transformation occurs at a high frequency. Non-homologous DNA may also be incorporated, but at a much lower frequency. In the laboratory, this attribute facilitates allelic replacement of wild-type genes with mutated ones

as well as allowing isolation and characterization of selected mutants (Collier et al., 1998; de Berardinis et al., 2008; Gregg-Jolly and Ornston, 1990; Hütler, N. and W. Wackernagel et al., 2008).

This natural and highly efficient transformation also makes *A. baylyi* an ideal organism for genetic engineering. The ability to incorporate genetic elements into the chromosome with ease allows much more stable constructions than providing the same elements *in trans*. This trait was exploited in the recent construction and preliminary application of a strain of *A. baylyi* capable of detecting salicylic acid. The recombinant biosensor strain was able to detect salicylic acid as a metabolic intermediate in cultures of *Pseudomonas putida* that degrade the polycyclic aromatic hydrocarbon pollutant, anthracene, as well as in tobacco leaves infected with tobacco mosaic virus (Huang et al., 2005; Huang et al., 2006).

### **LysR Type Transcriptional Regulators (LTTRs)**

LTTRs comprise the largest and most diverse family of prokaryotic transcriptional regulators and control a variety of cellular functions. LTTRs are not prevalent in the archaea, but they are in the proteobacteria and are predicted to encode approximately 20-30% of the regulators in many species (Craven et al., 2008). Typical LTTRs consist of approximately 280 - 350 amino acids and contain a highly conserved N-terminal winged helix-turn-helix (wHTH) motif as well as a more variable effector binding domain at the C terminus. In general, LTTRs positively regulate expression of their target genes in response to low molecular weight effectors and are negatively autoregulatory. The genes that encode LTTRs are commonly located directly upstream and divergently transcribed from genes they regulate. LTTRs are multimeric in solution, forming dimers or tetramers, and most respond to an effector molecule. The operator/promoter regions usually contain 2 - 3 regions of dyad symmetry; one very strong recognition site that binds the

regulator regardless of the presence or absence of an inducer and another site, the activation site, closer to the start of transcription of the target gene (Schell, 1993).

CbnR, the LTTR that regulates expression of the genes responsible for chlorocatechol degradation in the 3-chlorobenzoate degrading bacterium, *Ralstonia eutropha* NH9 has been structurally characterized as a full-length protein. The protein was crystallized as a tetramer in a biologically active form and the presence of a wHTH was confirmed (Muraoka et al., 2003). The wHTH motif is a variation on the typical tri-helical bundle that forms the foundation of the most common DNA-binding scaffold (Aravind et al., 2005; Brennan et al., 1993). A sharp bend exists between the second and third helices, and although this turn region is only a few residues in length, in some regulators it has been suggested to contact RNA polymerase directly, playing a crucial role in transcription activation (Jourdan and Stauffer, 1998; Lochowska et al., 2004). The third helix is considered the recognition helix and generally interacts with the major groove of the DNA. The wing may interact with the minor groove of the DNA, as has been shown for other proteins, but this remains to be established for LTTRs (Huffman and Brennan, 2002).

### **LTTRs & RNA Polymerase**

In general, bacterial transcriptional regulators interact with either  $\alpha$  or  $\sigma^{70}$  subunits of RNA polymerase, depending on the class of the promoter (Dove and Hochschild, 2005). Class I promoters interact with activators that bind upstream, greater than -35 from the start of transcription, of the RNA polymerase binding site. At Class II promoters, activators bind regions overlapping or adjoining the -35 element. Class III promoters usually interact with multiple activators that bind more than 90 bp upstream of the RNA polymerase binding site. Regulators of class I and III promoters generally bind the  $\alpha$  C-terminal domain of RNA polymerase, while regulators of class II promoters usually bind the  $\sigma^{70}$  subunit (Dove and

Hochschild, 2005). In the effector-bound, active form, BenM binds site 2 of the *benA* promoter which includes the -35 element, suggesting that this LTTR may interact with the  $\sigma^{70}$  subunit of RNA polymerase.

An activating region within the turn of the HTH DNA-binding motif has been identified in CysB, a LTTR responsible for regulating sulfur assimilation in *Escherichia coli* (Lochowska et al., 2004). Mutants carrying substitutions at key residues within the turn region were not inhibited in DNA binding, as indicated by electrophoretic mobility shift assay and DNase I footprinting, but they did display drastically reduced expression of a *lacZ* reporter gene. DNase I footprinting reactions also revealed weakened protection of the RNA polymerase binding site by turn region protein variants, suggesting that these changes resulted in an inability to position RNA polymerase on the DNA. Lochowska *et al* also performed extensive alanine scanning to determine the regions of the  $\alpha$  subunit of RNA polymerase that were involved in associating with CysB. Finally, they created a two-hybrid system (Dmitrova et al., 1998), combining CysB and the portion of the  $\alpha$  subunit thought to be responsible for associating with CysB. These studies indicated that alanine substitutions within either the turn region of CysB or residues 271-273, the  $\alpha$  C-terminal domain of RNA polymerase, disrupted recognition of the promoter and therefore regulation (Lochowska et al., 2004).

Another group has reported findings that the same position within this turn region is responsible for interactions with both the  $\alpha$  C-terminal domain and the  $\sigma^{70}$  subunit of RNA polymerase. Stauffer and Stauffer have shown that GcvA, the LTTR found in *E. coli* that regulates glycine cleavage genes, activates transcription from a class III promoter, *gcvTHP*, and from a class II promoter, *gcvB* (Stauffer and Stauffer, 2005). When the  $\alpha$  C-terminal domain of RNA polymerase was altered they noticed that activation was impacted at the *gcvTHP* promoter

but not at the *gcvB* promoter. When the level of transcription was measured with  $\sigma^{70}$  variants, the opposite effect was observed. Transcription was not inhibited at the *gcvTHP* promoter, but it was affected at the *gcvB* promoter. Substitutions at the same position within the turn of the LTTR resulted in loss of regulation at both promoters (Stauffer and Stauffer, 2005). These studies have begun to investigate the interactions between LTTRs and RNA polymerase. Further studies using various representatives will be needed before any generalizations can be made for the entire LTTR family.

### **LTTR Consensus Sequence Recognition & Protein-DNA Interactions**

The consensus recognition sequence for LTTRs is T – n11 – A within a region of dyad symmetry (Schell, 1993). The *benA* promoter contains three sites with this pattern: ATAC-N7-GTAT (hereafter referred to as site 1) from -71 to -57, ATAC-N7-GTGT (hereafter referred to as site 2) from -50 to -36, and ATTC-N7-GTAT (hereafter referred to as site 3) from -19 to -5, relative to the *benA* transcriptional start site (Figure 1.4) (Bundy et al., 2002). The current model for protein-DNA interactions at *benA* predicts that the regulatory protein binds to different sites on the DNA in the presence or absence of inducer(s), regulating transcription accordingly. DNase I footprinting experiments showed that in the absence of inducers, BenM binds sites 1 and 3 of the *benA* promoter, occluding RNA polymerase and repressing transcription. In the presence of muconate and benzoate, BenM shifts to sites 1 and 2, making the -10 promoter element available, possibly forming contacts with RNA polymerase, and activating transcription (Figure 1.4) (Bundy et al., 2002).

The interactions between many LTTRs and their target DNA have been well investigated and characterized. LTTRs exhibit a broad range of affinities for their target promoters. TsaR, an oxygen-sensitive LTTR that regulates *p*-toluenesulfonate in the bacterium *Comamonas*

*testosteroni* T-2, was reported to have a dissociation constant ( $K_d$ ) of  $9 \times 10^{-5}$  M for its target promoter without effector (Tralau et al., 2003). CatR, an LTTR that regulates expression of the genes responsible for catechol degradation in response to an inducer, muconate, in *Pseudomonas putida*, has a reported  $K_d$  of  $7 \times 10^{-11}$  M in the absence of inducer and  $3.1 \times 10^{-11}$  M in the presence of inducer (Parsek et al., 1994). PcaQ, the LTTR responsible for aromatic compound degradation in the legume endosymbiotic bacterium, *Sinorhizobium meliloti*, has a  $K_d$  for its target promoter of  $5.4 \times 10^{-8}$  M, consistent with the presence of a high-affinity interaction (MacLean et al., 2008).

The above binding constants were determined using the electrophoretic mobility shift assay technique (Lane et al., 1992). This method has been routinely and successfully used to determine protein-DNA interaction characteristics for a variety of complex types, including some LTTR-DNA interaction studies in *A. baylyi*. CatM has been shown to bind specifically to the *catM-catB* intergenic region as well as a region upstream of *catA* (Romero-Arroyo et al., 1995). Additionally, both BenM and CatM were shown to bind the *benP* promoter in the presence and absence of inducer (Clark et al., 2002). BenM and CatM have also been reported to bind the LTTR consensus sequence of the *pcaUI* operator-promoter region, and the affinity of CatM for the promoter was increased in the presence of muconate (Brzostowicz et al., 2003). DNA-protein interactions in *A. baylyi* have also been examined using the surface plasmon resonance method (Lalonde et al., 2008). The interaction between wild type and variant versions of PobR, an IclR family transcriptional regulator responsible for activating expression of the genes necessary to metabolize *p*-hydroxybenzoate, and its target promoter, *pobA*, were compared using this method. Only qualitative measurements were made during this study, yet PobR variants exhibited clearly different binding characteristics relative to wild type (Kok et al., 1998).

Another method of analyzing the affinity of DNA-protein interactions is fluorescence polarization or fluorescence anisotropy (Jameson and Crooney, 2003). This method has many advantages over both gel shifts and surface plasmon resonance. First, a variety of interaction conditions may be analyzed with relative ease, including those that are not compatible with the previously mentioned methods. Also, a great size difference among complex components is not required in order to determine an equilibrium constant using this method. Finally, this method allows analysis of all components in solution, providing a true equilibrium constant as well as requiring comparatively simple equipment (Lundblad et al., 1996).

The fluorescence anisotropy method detects changes in the rotational motion of fluorescent molecules in solution. Because fluorescent molecules favor light absorption in a particular plane, it is possible to detect depolarization of emitted light. Extrinsic depolarization, the depolarization that occurs throughout the excited state of the fluorescent molecule, is most affected by complex formation and therefore forms the foundation for quantifying rates of association. Because of their mobility in solution, small molecules typically have greater rotational motion and, therefore, greater fluorescence polarization than larger molecules. If a molecule rotates rapidly with respect to the fluorescence lifetime, then anisotropy will approach zero and if a molecule rotates slowly, then anisotropy will approach the limiting value. As rotation increases, anisotropy decreases and as rotation decreases, anisotropy increases. Therefore, the anisotropy of a complex will increase as molecules associate (Lundblad et al., 1996). The many benefits of this method combined with the absence of binding constants for any of the LTTR-DNA interactions governing the *ben* and *cat* operons in *A. baylyi*, lead to the design of a series of experiments to address these issues.

## Regulation of *benA* in the Absence of BenM

As described earlier, BenM-mediated regulation of the *ben* genes is required for growth on benzoate. However, some strains acquire the ability to grow on benzoate as the sole carbon source in the absence of BenM. Several mechanisms that restore growth in the absence of BenM have been identified. Some mutations in the *benA* promoter region elicit high level expression of the *ben* genes without a regulator (Collier et al., 1998). Other mutations in the *benA* promoter region allow muconate-induced, but not benzoate-induced, expression of the *ben* genes by CatM (Collier et al., 1998). Mutations in *catM* that result in increased expression of *benA* in response to muconate have also been isolated (Ezezika et al., 2006). Mutations have also been observed in *catB* and are predicted to affect the intracellular concentration of muconate and therefore the activation of the *ben* genes by CatM (Casper et al., 2000). Finally, some as yet uncharacterized mutations have been found in the *catMB* intergenic region (Lauren Collier, 2000; Sandra Haddad, Chelsea Kline and Jennifer Morgan, unpublished data).

For the purposes of this study, the mutations in *catB*, the gene encoding muconate cycloisomerase, are especially interesting because it is likely that the recently isolated strains with mutations in the *catMB* intergenic region characterized in this thesis are operating via a similar mechanism: by altering the intracellular concentration of muconate (Figure 1.5). To locate the original mutations that allow BenM-independent growth on benzoate, regions of DNA from the mutants were captured using the gap repair method (Gregg-Jolly and Ornston, 1990). This method is another example of capitalizing on the natural and high-efficiency transformation of *A. baylyi*. Gap repair involves using a linearized plasmid containing homology to either side of a chromosomal region of interest to transform a strain of interest. Homologous recombination occurs *in vivo*, capturing the genes between the homologous regions and allowing the plasmid to

form a circle or “repair the gap.” The plasmid can then be extracted, subcloned, and sequenced. In earlier studies, the *cat* region was a predicted site for mutation. Therefore, a plasmid contained part of ORF1 and ORF2 at one open end and part of *catJ* and *catFD* at the other, allowing *catM* and *catB* to be captured. Once isolated the plasmids were digested with restriction enzymes, resulting in fragments containing *catM* only, *catB* only, and the *catMB* intergenic region. The fragments were used to transform the parent strain that lacked a functional BenM, and those that restored the ability to grow on benzoate as a sole carbon source were sequenced (Collier, 2000).

Those fragments that restored the ability to grow on benzoate in strains containing a disrupted *benM* were further characterized. Four different substitutions in CatB were discovered: an arginine to leucine at position 198, an arginine to cysteine at position 99, a proline to serine at position 328, and a 9bp insertion (TTCAACAGC) which encodes two additional glutamine residues and one additional leucine between positions 209 and 210 (Cosper et al., 2000). In each of these strains the specific activity of CatB was reduced compared to wild type and the specific activity of CatA was increased compared to wild type. This result suggests that the substitutions in CatB make it less effective for converting muconate to muconolactone, increasing the intracellular concentration of muconate. This increase in intracellular muconate may then increase expression at *catA*. When grown in rich medium and induced with muconate, the *catB* mutants exhibited *benA* expression that was less than wild type, but greater than that observed in a strain with a disrupted *benM*. Like benzoate, anthranilate is degraded through the catechol branch of the  $\beta$ -ketoacid pathway. Therefore, strains with less efficient CatB enzyme may accumulate intracellular muconate during growth on anthranilate. When grown on anthranilate, the *catB* mutants approached or exceeded wild-type expression of *benA*. Because *catA*

expression is also increased under high muconate concentrations, and the mutations in *catB* make the enzyme less efficient, it is possible to imagine a model that allows CatM activation of the *ben* genes in response to increased intracellular concentration of muconate (Figure 1.5) (Cosper et al., 2000).

It is known that the *catB* mutants grow on benzoate and exhibit decreased specific activity of CatB, but it remains to be proven experimentally that the proposed regulatory model is responsible for the phenotype. Ideally, measurements of intracellular muconate could be made and used to support the model. Although attempted in the previous CatB study, no significant difference between wild-type and mutant muconate concentration could be detected by high performance liquid chromatography in the culture supernatant. Discerning differences in internal and external concentration of muconate is difficult. First, only small amounts of muconate could accumulate because concentrations above 1 mM are toxic (Gaines III et al., 1996). Comparison of wild-type and mutants is also complicated because the mutants have longer lag phases and growth rates, making it difficult to compare points in the growth cycles. Uncertainties about the import and export of muconate also make it difficult to conclude anything about its presence within the cell. However, it is known that muconate elicits different physiological effects when it is provided exogenously as opposed to endogenous generation (Gaines III et al., 1996). Studies of strains with mutations in the *catB* promoter region may provide more evidence in support of the regulatory model shown in Figure 1.5.

### **Summary of Studies for this Project**

A number of independent, spontaneous mutations in the *catB* promoter region have been isolated and shown to restore growth on benzoate as a sole carbon source in the absence of BenM by previous lab members including, Lauren Collier and Sandra Haddad, but they were not

characterized. This study focuses on characterizing these mutations and determining how they compensate for the loss of BenM-mediated regulation. Based on the model developed for the *catB* gene mutants, we predict that mutations in the *catB* promoter decrease expression of the *catB* promoter, resulting in an increase in intracellular muconate and ultimately allowing muconate-induced CatM-activated expression of *benA*. First, the specific activity of CatA, catechol dioxygenase, and CatB, muconate cycloisomerase, was determined and compared to the results of the *catB* mutants and the wild-type strain. Next, expression at *benA* was measured using beta-galactosidase assays with transcriptional reporter gene fusions and compared to wild type and BenM-disrupted control strains. High performance liquid chromatography was used to determine the concentration of metabolites, specifically muconate, in the culture supernatants of wild-type and mutant strains. Finally, fluorescence polarization was used to assess the affinity of protein-DNA interactions between CatM and the wild-type and mutant promoters.

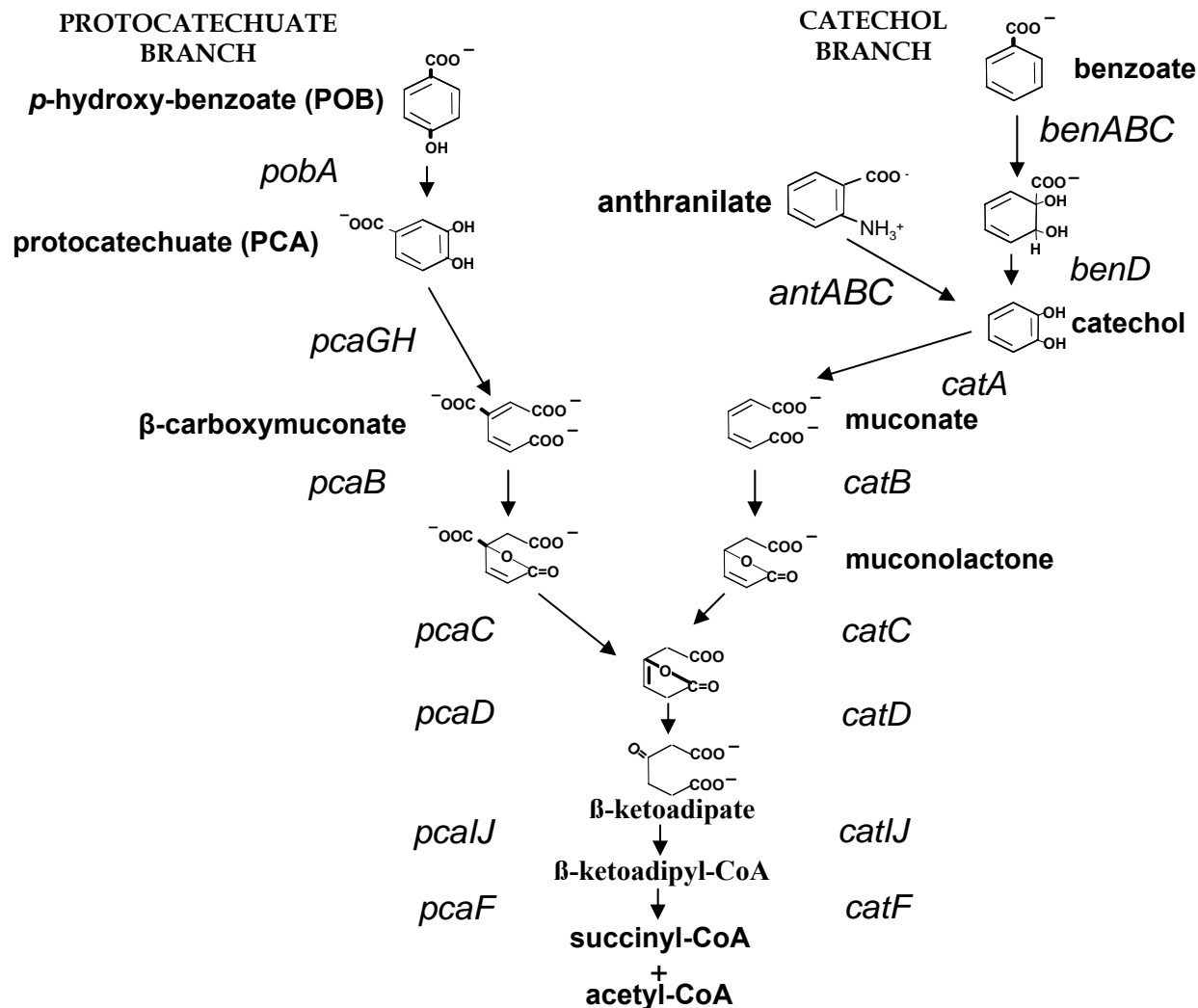


**Figure 1.1** The  $\beta$ -ketoadipate pathway in *A. baylyi* ADP1. Aromatic compounds are degraded through either the catechol or protocatechuate branch of the pathway. Genes encoding the enzymes of the pathway are listed alongside the reactions they perform (adapted from Harwood and Parales, 1996).

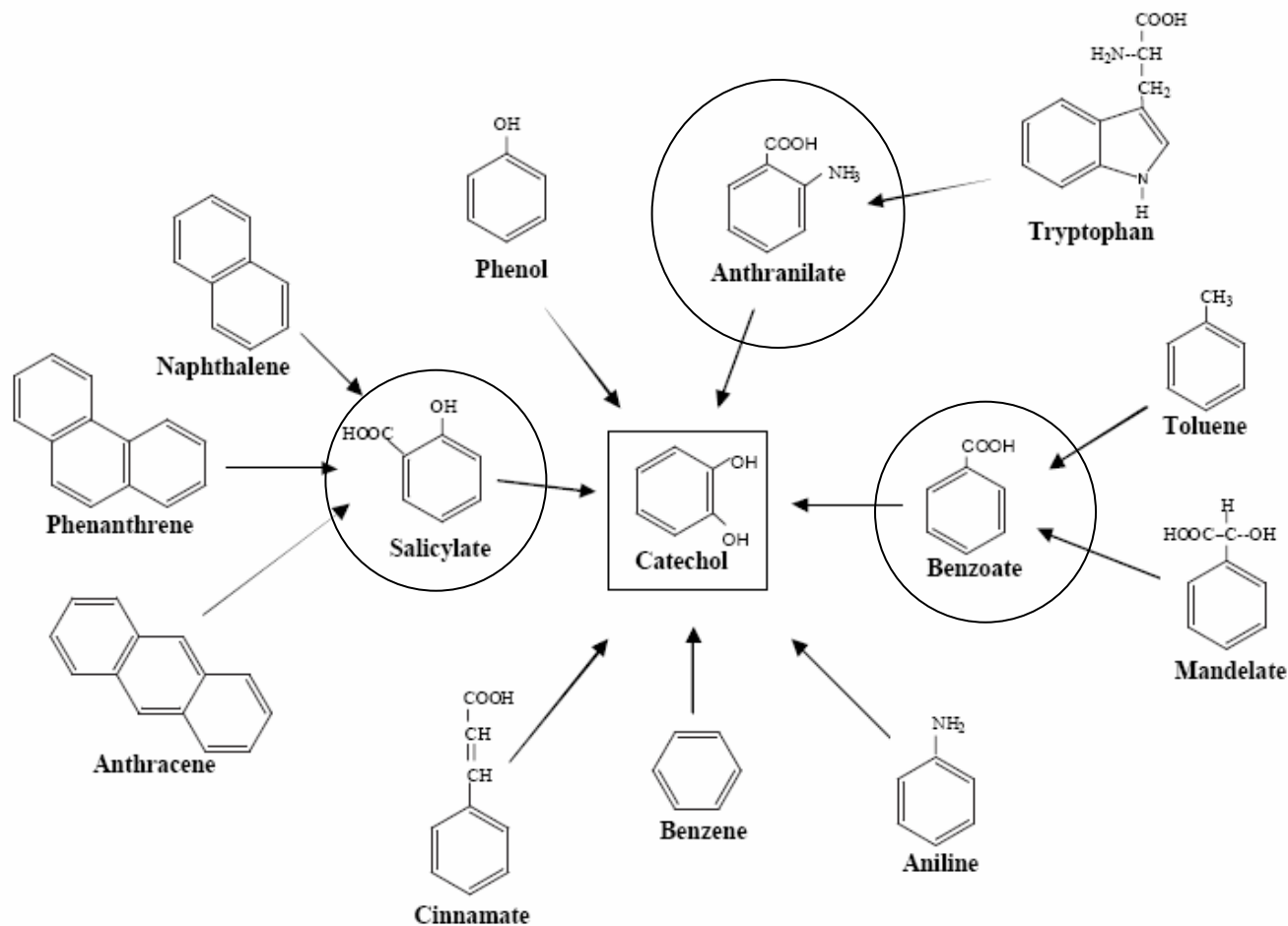


**Figure 1.2 Common aromatic compounds dissimilated by microorganisms via the intermediate catechol and the  $\beta$ -keto adipate pathway (adapted from Harwood and Parales, 1996).** Although *A. baylyi* ADP1 does not degrade all compounds presented here, it does degrade the common intermediates, anthranilate, benzoate, and salicylate (enclosed in circles) and is an excellent model for studying degradation of these compounds.

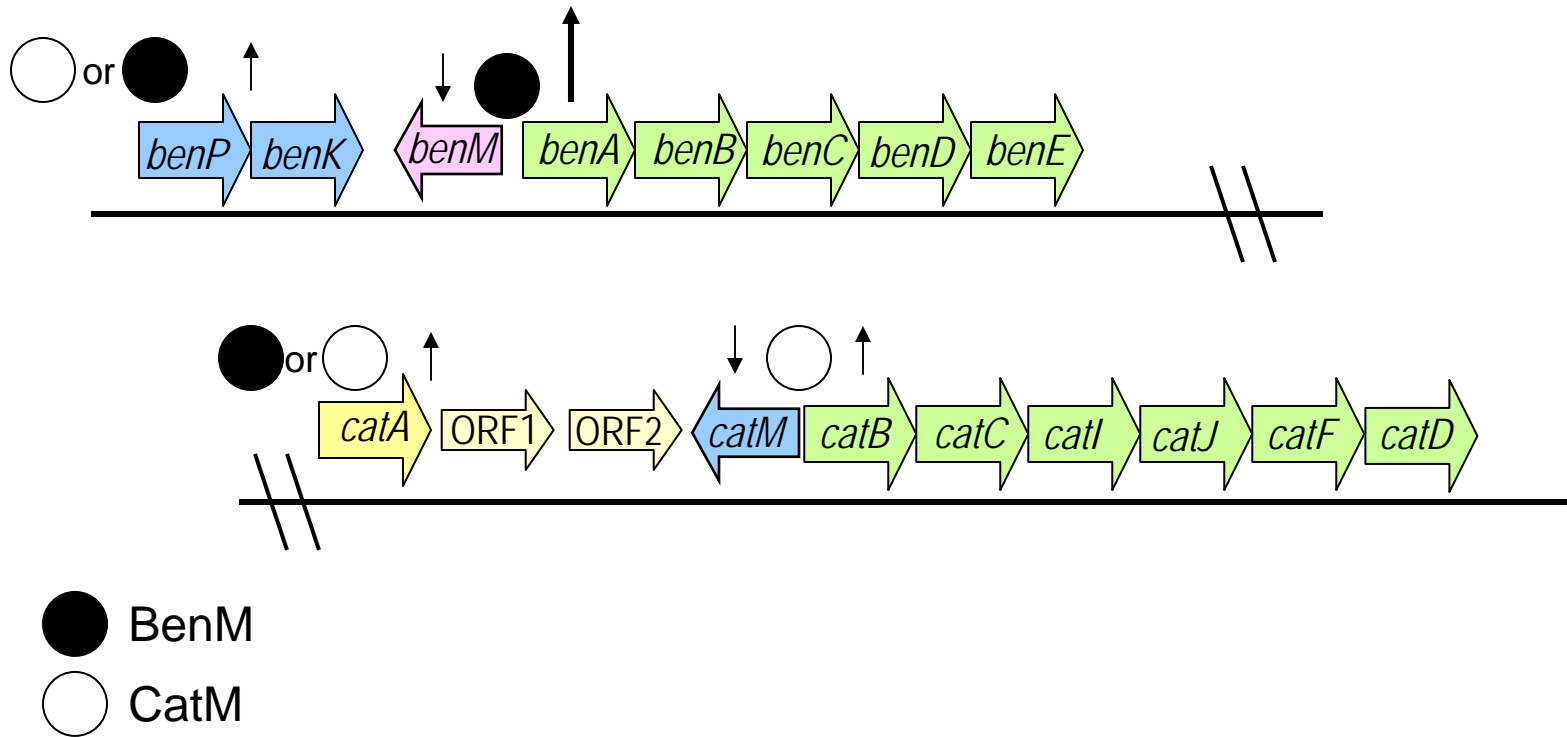


**Figure 1.3 Regulation of the *ben* and *cat* regions by BenM and CatM.** The closed circles represent BenM, which is capable of activating transcription at *catA*, *benP*, and *benA* in response to its inducers. Activation at *benA* occurs synergistically in response to two effectors, benzoate and muconate (indicated by larger up arrow). The open circles represent CatM, which is capable of activating transcription at *catA*, *benP*, and *catB* in response to muconate as an effector. CatM and BenM are also negatively autoregulatory as indicated by down arrows. CatM can activate low-level expression of *benA* and BenM can activate low-level expression of *catB*, but not enough to permit growth.

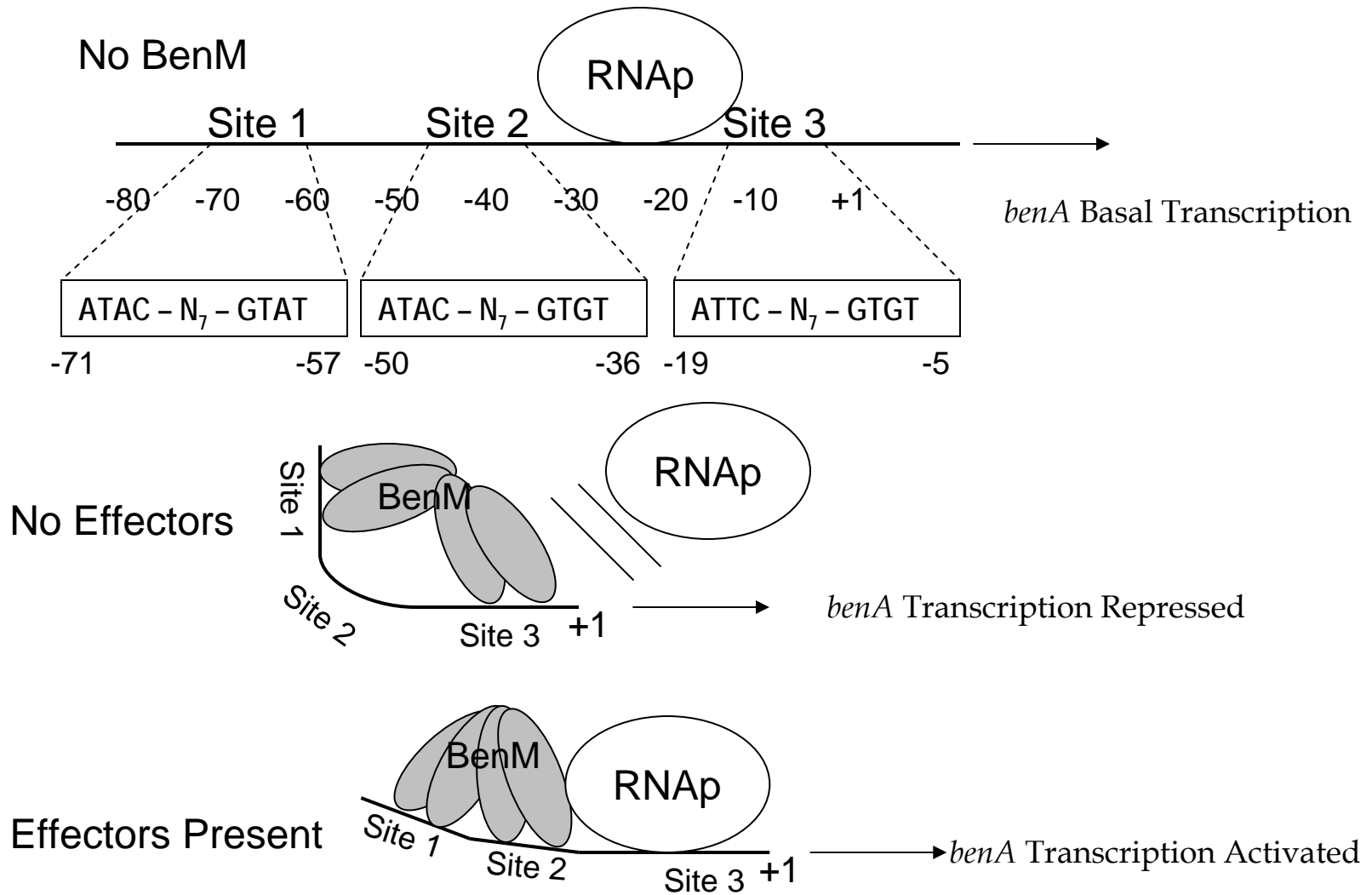


**Figure 1.4 Regulatory model of the *benA* promoter adapted from Bundy 2001.** BenM binds to sites 1 and 3 without inducers, repressing transcription. When effectors are present, BenM binds sites 1 and 2 and activates transcription. Each smaller gray oval represents one molecule of BenM that oligomerizes to form tetramers and the larger white ovals labeled RNAP represent RNA polymerase.

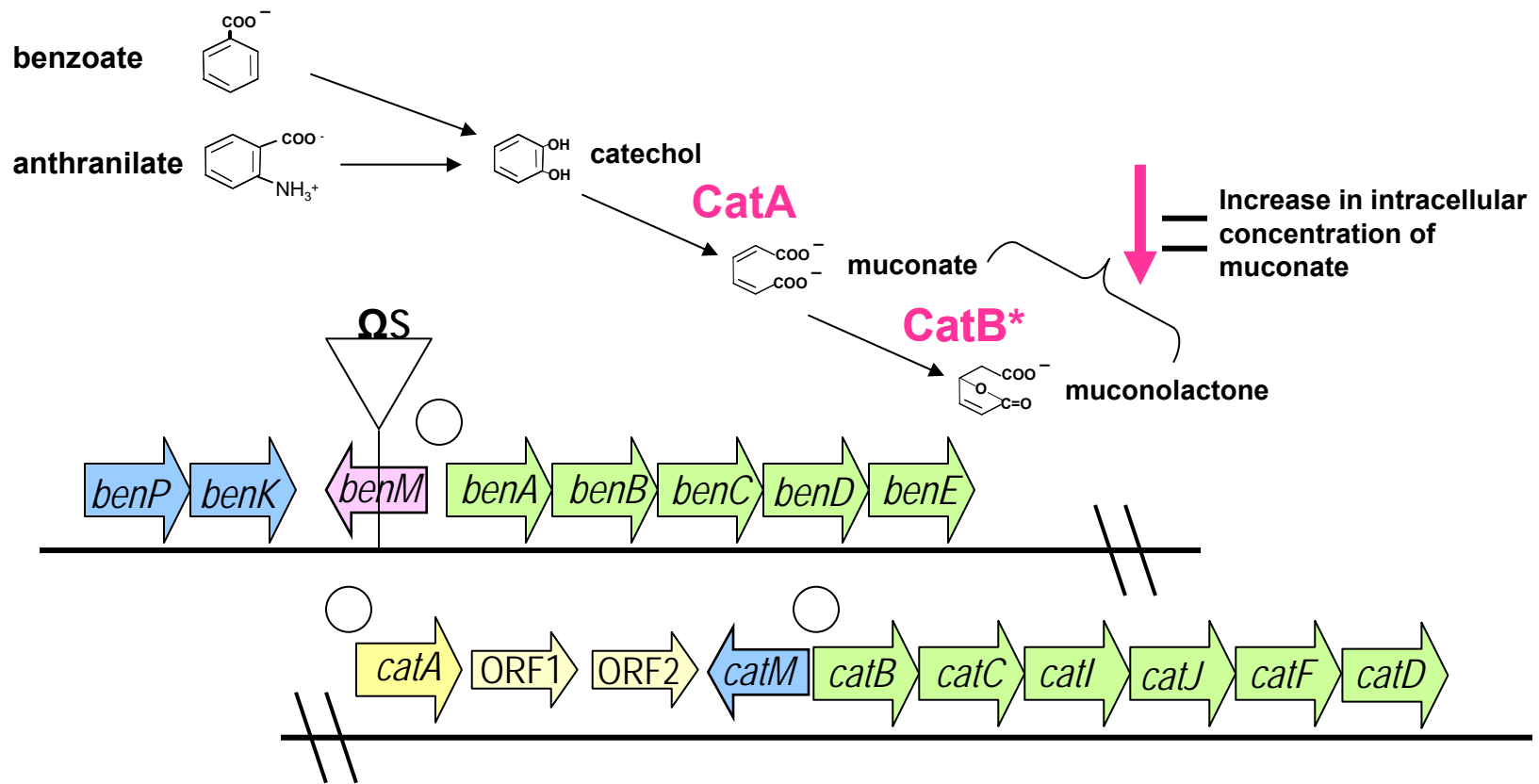


**Figure 1.5 Proposed model of CatM-activated expression of *benA* in response to increased intracellular concentration of muconate.** Mutations in *catB* decrease the specific activity of the enzyme (Cosper et al., 2000). Presumably, this reduced enzyme activity results in less muconate being converted to muconolactone. Enough muconate should accumulate to allow CatM to activate expression of the *benA* promoter. Open circles represent CatM regulatory protein at the various promoters.

## CHAPTER II

TRANSCRIPTIONAL REGULATION OF THE *catB* OPERATOR-PROMOTER:  
CatM-MEDIATED EXPRESSION OF THE *benA* PROMOTER IN RESPONSE TO  
INCREASED INTRACELLULAR MUCONATE

## INTRODUCTION

### Regulation of *ben* and *cat* genes

In *Acinetobacter baylyi*, the genes involved in benzoate degradation are regulated by two homologous LysR-type transcriptional regulators: BenM and CatM. These regulatory proteins are 59% identical and 75% similar in amino acid sequence. Although they are similar in sequence, they are diverse in regulatory function. BenM regulates gene expression at the *benA* promoter, responding synergistically to two effectors, benzoate and muconate. CatM is responsible for regulation of the *catB* promoter, and responds to only one effector, muconate. Either regulator is sufficient to activate transcription of the *benP* and *catA* promoters (Bundy, 2001; Clark et al, 2002; Collier et al. 1998; Romero-Arroyo et al., 1995). However, BenM cannot replace CatM and neither can CatM replace BenM for expression of the *benA* and *catB* promoters, respectively (Figure 2.1) (Ezezika et al., 2006). Analysis of the effector binding domain crystal structure of BenM identified amino acid residues critical for interacting with benzoate (Ezezika et al., 2007). Replacing these residues in the benzoate binding site with the amino acid from the corresponding position in CatM abolishes *benA* activation in response to benzoate (Craven, 2009). The DNA binding domains as well as the promoter sequences are also similar, but less is known about the key differences in these elements that lead to the specificity of regulation.

### Mutations that allow growth on benzoate as a sole carbon source in the absence of BenM

Previous studies seeking to identify mutations and conditions that allowed growth on benzoate as a sole carbon source in the absence of a functional BenM revealed several components that

contribute to the complex regulation of these genes. Mutations were identified in the *benA* promoter (Collier et al., 1998), the CatM regulatory protein (Ezezika et al., 2006), the muconate cyclisomerase enzyme, CatB (Casper et al., 2000), and the *catMB* intergenic region (Lauren Collier, 2000; Chelsea Kline, Jennifer Morgan and Sandra Haddad, unpublished data). The mutations in the *catB* structural gene are proposed to permit growth on benzoate in the absence of BenM by increasing the intracellular concentration of muconate enough to allow CatM to activate the *benA* promoter (Figure 2.2) (Collier, 2000; Casper et al., 2000). The recently identified mutations in the *catB* promoter are the focus of this study. Characterization of these mutants may support the previous model of CatM-mediated *benA* expression as well as increase understanding of the role of the *catB* promoter and metabolites in the overall regulatory scheme.

### **Isolation of *catMB* intergenic region mutants**

These mutants arose as spontaneous mutations in strains lacking a functional BenM. Briefly, ISA36 (*benM* disrupted with  $\Omega$  streptomycin/spectinomycin cassette) was grown on minimal medium plus benzoate and spontaneous *ben*<sup>+</sup> colonies appeared. The gap repair method developed by Gregg-Jolly and Ornston was used as previously described to capture 5.25 kb of chromosomal DNA including *catM* through *catI* (Collier et al., 1998; Gregg-Jolly and Ornston, 1990). Fragments from this region were used to transform the parent strain, ISA36, and those that restored growth on benzoate were sequenced. Two independent mutants contained an identical insertion of one T between positions -66 and -62, relative the *catB* transcriptional start site. This corresponds to the space between the ATAC-N<sub>7</sub>-GTAT LTTR consensus sequence in site 1 of the *catB* promoter, changing it to ATAC-N<sub>8</sub>-GTAT (ACN150 and ACN154) (Collier,

2000). Another mutation, a C to A change at position -46, relative the start of *catB* transcription, was also isolated (ACN724) (Chelsea Kline and Jennifer Morgan, unpublished data).

Additional mutations in the *catB* promoter were derived from a different parent strain. This strain was originally constructed for another project and therefore has unique genetic components. An earlier study indicated that the anthranilate dioxygenase, encoded by *antABC*, was capable of converting benzoate to benzoate diol *in vitro* (Eby et al., 2001). It was later hypothesized that a strain containing the *antAB* genes in place of the *benAB* genes might be able to grow on benzoate. The strain necessary to investigate this was constructed by first deleting the *antAB* genes from their native locus as well as deleting the *benAB* genes. Finally, the *antAB* genes were inserted to replace the *benAB* genes, but remained under control of the native *benA* promoter. Ultimately, these strains were not able to grow on benzoate as a sole carbon source, but they did maintain the ability to grow on anthranilate. Because the *antAB* genes were under control of BenM, regulation could be disrupted by interrupting the BenM regulatory protein. In a manner similar to the isolation of the mutants derived from ISA36, spontaneous mutants that regained the ability to grow on anthranilate in the absence of a functional BenM were isolated. The insertion of one T in site 1 of the *catB* promoter was again isolated (ACN651). A mutation changing a C to T was identified in two independent strains at the same -46 position, relative to the *catB* transcriptional start site, corresponding to the predicted site 2 of the *catB* promoter (ACN645 and ACN647). Finally, a T to C change was isolated at position -49, relative to the start of *catB* transcription, which is also within the predicted site 2 (ACN649) (Sandra Haddad, unpublished data). The location, strain name and allele number of all mutations is indicated in Figure 2.3.

## **Characterization of *catMB* intergenic region mutants**

The mutations in the *catB* structural gene are proposed to permit growth on benzoate in the absence of BenM by increasing the intracellular concentration of muconate enough to allow CatM to activate the *benA* promoter (Collier, 2000; Cosper et al., 2000). The recently identified mutations in the *catB* promoter are hypothesized to be operating via a similar mechanism. Characterization of these mutants may support the previous model of CatM-mediated expression of the *benA* promoter as well as determine the contribution of the *catB* promoter and metabolites formed by the *catBCIJFD* gene products in the overall regulatory scheme.

## **MATERIALS AND METHODS**

### **Bacterial strains, plasmids, and growth conditions**

*Acinetobacter* strains (Table 2.1) were derived from *Acinetobacter baylyi* strain ADP1, previously designated as BD413 (Juni, E. and A. Janik, 1969). Bacteria were cultivated in minimal medium plus a carbon source or Luria-Bertani (LB) broth with agitation at 37 °C. The minimal medium contained 12.5 mM potassium dihydrogen phosphate (KH<sub>2</sub>PO<sub>4</sub>), 12.5 mM dibasic sodium phosphate (Na<sub>2</sub>PO<sub>4</sub>), 0.1% ammonium sulfate ((NH<sub>4</sub>)<sub>2</sub>SO<sub>4</sub>), and 0.1% concentrated base, pH 6.9. The concentrated base solution included 10 g nitrilotriacetic acid, 30 g magnesium sulfate (MgSO<sub>4</sub>), 2.5 g calcium chloride (CaCl<sub>2</sub>), 9.25 g ammonium molybdate ((NH<sub>4</sub>)<sub>6</sub>Mo<sub>7</sub>O<sub>24</sub> 4H<sub>2</sub>O), 100 g ferrous sulfate (FeSO<sub>4</sub>) and 50 mL Hutners metals 44 (Cohen-Bazire, G. et al., 1957). Carbon sources were supplied at the following final concentrations: 2 mM anthranilate, 2 mM benzoate and 10 mM succinate. When necessary, antibiotics were included at the following final concentrations: ampicillin, 150 µg/mL, kanamycin, 25 µg/mL,

streptomycin, 12.5 µg/mL, and spectinomycin, 12.5 µg/mL. *Escherichia coli* DH5α (Invitrogen) served as a plasmid host.

### **Determining bacterial growth rates**

For growth curves, LB plus the appropriate antibiotic-grown cells were used to inoculate 5-mL overnight cultures of LB plus 2 mM anthranilate or benzoate or minimal medium plus 10 mM succinate. The following morning, 1 mL of the overnight culture was used to inoculate 100 mL of minimal medium plus 2 mM anthranilate or benzoate or 10 mM succinate as the sole carbon source. Growth was observed turbidometrically using a Klett-Summerson colorimeter or spectrophotometrically at 600 nm. Generation times were calculated by plotting the data using Prism software and fitting the curves by a linear regression such that the generation time equaled the amount of time necessary for cell density to double during the exponential growth phase.

### **Determining metabolite concentration using high-performance liquid chromatography**

Samples from cultures growing on anthranilate were taken at timed intervals, and whole cells were removed by filtration using a 0.2 µm polyethersulfone membrane (Whatman). From each time point, 10 µL of cell-free culture media was separated on a C18 reverse-phase column (Restek). The flow rate was 1 mL/min and the mobile phase was 30% acetonitrile (CH<sub>3</sub>CN) plus 0.1% phosphoric acid (H<sub>3</sub>PO<sub>4</sub>). The presence of benzoate, anthranilate, catechol, and muconate was observed by UV detection at 260 nm. The retention times for benzoate, anthranilate, catechol, and muconate were 9.6, 6.5, 5.2, and 3.5 minutes, respectively. A serial dilution of benzoate or anthranilate, catechol, and muconate ranging from 0.00125 – 2 mM was used to calibrate the equipment daily. Peak areas corresponding to these external standards were used to

generate a standard curve and experimental samples were quantified using the Shimadzu software package.

### **Preparation of crude cell extracts and measurement of catechol 1,2-dioxygenase (CatA) and muconate cycloisomerase (CatB) specific activities**

Cultures were grown in 50 – 100 mL of minimal medium plus 2 mM anthranilate as the sole carbon source until early stationary phase. Cells were harvested by centrifugation at 10,000 rpm for 10 min, washed in 1 mL breaking buffer and pelleted, resuspended in 400  $\mu$ L breaking buffer and disrupted by sonication (10 – 3s bursts). The breaking buffer contained 10 mM ethylenediamine dihydrochloride and 1  $\mu$ M manganese chloride ( $\text{MnCl}_2$ ), adjusted to pH 7.3 (Meagher et al., 1990). Cellular debris was removed by centrifugation at 15,000 rpm for 5 min and the crude cell extract was retained. CatA activity was measured in an assay buffer containing 33 mM Tris-HCl (pH 7.5), 20  $\mu$ M catechol, and 1 mM ethylene diamine tetraacetic acid (EDTA). CatB activity was measured in an assay buffer containing 33 mM Tris-HCl (pH 8.0), 1 mM  $\text{MnCl}_2$ , and 100  $\mu$ M muconate. Protein concentration was determined using the Bradford method with bovine serum albumin (BSA) as the standard (Bradford, 1976). The activities of catechol 1,2-dioxygenase (CatA) and muconate cycloisomerase (CatB) were measured spectrophotometrically by the increase or decrease in muconate concentration, respectively, as determined by absorbance at 260 nm (Meagher et al., 1990; Ngai et al., 1990).

### **$\beta$ -Galactosidase (LacZ) assays**

Strains derived from ISA36 were transformed with restriction enzyme Asp718 linearized pBAC54a, generating *benA::lacZ* reporter strains. Strains derived from ACN620 were

transformed with Asp718 linearized plasmid, pBAC162, generating *antA::lacZ* reporter strains. Cultures were grown overnight in 5 mL of LB, LB plus 3 mM benzoate or LB plus 3 mM muconate. To lyse the cells, 50  $\mu$ L of culture were combined with 400  $\mu$ L of Z Buffer (0.1% SDS,  $\beta$ -mercaptoethanol) and 50  $\mu$ L chloroform and vortexed for 10 seconds. Assays were performed according to the FluorAce  $\beta$ -Galactosidase reporter kit directions (BioRad). Briefly, 100  $\mu$ L of the disrupted cell mixture was combined with 100  $\mu$ L of kit-supplied assay buffer plus  $\beta$ -mercaptoethanol and 4-methylumbelliferyl  $\beta$ -D-galactopyranoside (MUG). Reactions were incubated at 37 °C for exactly 15 minutes. Reactions were stopped by adding 200  $\mu$ L of kit-supplied stop buffer.  $\beta$ -galactosidase cleavage of MUG results in a fluorescent product, 4-methylumbelliferone (4MU). Fluorescence was measured using a TD-360 minifluorometer (Turner Designs). Nanomoles of product were converted to enzyme activity units using the following equation  $\text{nmol}/(\text{vol} \times \text{time} \times \text{OD})$ .

### **Electrophoretic Mobility Shift Assay (EMSA)**

The full-length histidine-tagged CatM used during these experiments were purified by Amer Alanazi as previously described (Ezezika O. C. et al., 2007). Promoter DNA sequences were prepared by polymerase chain reaction (PCR) amplification of the wild-type and mutant *catB* promoter regions, using the primers *catB\_low* (5' CATCTTCTTTTCAATAAATAC 3'), *catM\_bind* (5' TATACGCCCTAATTGGT 3'), and Phusion<sup>TM</sup> high-fidelity DNA polymerase. PCR products were purified using the Qiagen QIAquick PCR purification kit and quantified by absorbance at 260 nm. PCR products were also cloned into the pCR2.1<sup>®</sup>-TOPO vector using the TOPO TA cloning kit (Invitrogen) (Table 2.1). Six percent polyacrylamide gels were prepared using ProtoGel polyacrylamide, Rhinohide gel strengthener, and 0.5X TBE. The mixture was

degassed by stirring under a vacuum for fifteen minutes. Polymerization was initiated with 10 % ammonium persulfate and tetramethylethylenediamine (TEMED). To determine in the interaction between CatM and the wild-type and mutant *catB* promoters, binding reactions were performed as follows. Increasing concentrations of CatM protein from 100 – 800 ng were added to separate binding reactions. The reaction buffer contained 10 mM Tris (pH 7.5), 1 mM EDTA, 50 mM KCl, and 5 mM DTT, plus 200 ng of wild-type or mutant promoter DNA. The reactions were incubated for 45 minutes at 37 °C. The reaction mixtures were loaded onto the gel and electrophoresed at 200 V for 45 minutes. The gel was stained with ethidium bromide and imaged.

### **Fluorescence Polarization**

The full-length histidine-tagged BenM and CatM used during these experiments were purified by Ajchareeya (Miki) Ruangprasert. Briefly, cell pellets containing either BenM or CatM were resuspended in binding buffer (30 mM Tris base pH 7.9, 500 mM NaCl, 5 mM imidazole, 10 mM BME, and 30 % glycerol) and applied to a metal chelate column. The proteins were eluted in buffer containing 30 mM Tris base (pH 7.9), 500 mM NaCl, 500 mM imidazole, 10 mM BME, and 30 % glycerol. Further purification of full-length CatM was not possible due to the tendency of the protein to precipitate. Additional purification of BenM was performed using a Q column. The Q start buffer contained 30 mM Tris base (pH 9), 50 mM NaCl, 250 mM imidazole, 10 mM BME, and 10 % glycerol. The protein was eluted with a buffer containing 30 mM Tris (base pH 9), 1 M NaCl, 250 mM imidazole, 10 mM BME, and 10 % glycerol.

Fluorescent polarization experiments were performed with a PanVera Beacon Fluorescence Polarization System. Unpurified oligonucleotides encompassing the promoter

DNA and fluorescein-labeled at the 5' end nearest site 1 were purchased from Sigma. Promoter sequences, predicted protein binding sites, mutations, and labels are summarized in Table 2.2. The oligos were resuspended in 10 mM cacodylate to approximately 1 mM concentration of DNA, and stored at 4 °C protected from light. Hybridization was performed by combining equimolar amounts of the labeled probes and complementary sequences to a final concentration of 50  $\mu$ M DNA in a total volume of 100  $\mu$ L sterile water. The reaction mixture were heated to 95 °C in a thermocycler for five minutes and cooled to room temperature gradually, allowing annealing to occur. The binding buffer contained 20 mM HEPES (pH 7.5), 150 mM NaCl, 1 mM DTT, and 5  $\mu$ g poly (dI-dC) to combat nonspecific binding. The labeled target promoter was present at a concentration of 0.5 nM in the binding reaction, and increasing concentrations, ranging from 0 – 150 nM, of either BenM or CatM were serially titrated into the binding reaction. Binding reactions were incubated at room temperature for 15 seconds to allow complex formation to reach equilibrium. After each addition of protein, polarization was measured three times. Samples were excited at 490 nm and emission was measured at 510 nm. The binding curves were fit by a nonlinear least squares regression analysis such that the dissociation constant ( $K_d$ ) equals the protein concentration at half maximal DNA binding (Shumacher M. A. et al., 2002 and Cardinaux J. et al.,2000).

## RESULTS

### Growth rates

Although strains with mutations in the *catB* promoter do grow on benzoate or anthranilate, it was necessary to compare the rate of growth with that of wild type. When grown on succinate, the *catB* promoter mutants did not exhibit significantly different doubling times compared to wild

type. However, when grown on benzoate or anthranilate, the strains did grow more slowly than wild type and some also had a significantly longer lag phase than wild type, ranging from eight to twenty-four hours (Table 2.3). The consistent growth rate on succinate among wild-type and *catB* promoter mutant strains suggests that neither the parent strain construction nor the spontaneous mutations have additional effects on cellular function under these conditions. Because the expression of the *ben* genes in response to increased intracellular muconate is not predicted to be equal to wild-type expression, the slower growth rate on benzoate and anthranilate is also expected. Finally, the extended lag phase in many of these strains provides additional support for the proposed *catB* regulatory model. If the strains only grow on benzoate and anthranilate once intracellular muconate reaches an increased concentration, then the lengthy lag phase may correspond to the length of time necessary for the cells to accumulate enough intracellular muconate to allow CatM-activated expression of the *benABCDE* operon.

### **Metabolite Concentration**

If the mutations do lead to an increase in intracellular muconate, then differences in metabolite concentrations between wild type and mutants may be detected. The consumption of aromatic carbon sources and the presence of metabolic intermediates was measured using high performance liquid chromatography. Cultures of wild-type cells grown on minimal medium plus 2 mM anthranilate consumed anthranilate and generated the intermediate, muconate, at rate consistent with the growth pattern (Figure 2.4). Cultures of *catB* promoter mutant cells also consumed the aromatic carbon source, anthranilate, and produced muconate. Although a significant increase in muconate concentration in the culture supernatant was not detected for all mutants, the mutants do exhibit a much longer lag phase and longer generation time (Figure 2.4).

This growth pattern is consistent with the idea that the mutants initially depend on basal level transcription of the *benA* promoter and cannot begin growing on the aromatic carbon source until enough muconate accumulates intracellularly to allow CatM-mediated expression of *benA*.

### **Specific Activity of CatA and CatB**

Because previously isolated mutations in the *catB* gene lead to an increased ratio of CatA to CatB activity and the *catB* promoter mutations were thought to be restoring growth in a similar way, the enzymatic activity of the *catMB* mutants was assayed. The effect of the *catB* promoter mutations on *cat* gene expression was assessed by determining the specific activity of catechol dioxygenase (CatA) and muconate cycloisomerase (CatB) in crude cell extracts of benzoate or anthranilate grown cultures. As mentioned earlier, the *catB* promoter strains grow more slowly, but they do ultimately grow, indicating that *catB* is expressed and functional. Previous studies reported that the ratio of CatA to CatB specific activity was approximately one to one (Casper et al., 2000). The present study also found CatA and CatB specific activities to be essentially equal in the wild-type strain with a ratio of 1.2 (Figure 2.6).

Like the previously characterized *catB* mutants, the *catB* promoter mutants also exhibited increased CatA activity and decreased CatB activity, resulting in higher ratios of CatA to CatB activity. Two mutants containing an insertion of one T in site 1 of the *catB* promoter, ACN150 and ACN651, and both strains containing mutations in the predicted site 2 of the *catB* promoter, ACN647 and ACN649, exhibited higher CatA specific activity, ranging from four to seven times greater than that of wild-type (Figure 2.5). All *catB* promoter mutants also displayed CatB specific activity that equaled only 26 – 57% of typical wild-type activity (Figure 2.6). The

increase in CatA activity combined with the decrease in CatB activity resulted in significantly increased ratios of CatA to CatB activity (Figure 2.6).

### **Expression of *benA* in *catB* promoter mutants**

The *catB* promoter mutants are capable of growth on benzoate or anthranilate as a sole carbon source in the absence of a functional BenM, suggesting that the mutations allow expression of the *benA* promoter. To assess expression at the *benA* promoter, reporter strains were constructed containing a *benA::lacZ* or an *antA::lacZ* fusion. Plasmid pBAC54a was linearized and used to transform strain ACN150, replacing the wild-type *benA* gene with the *benA::lacZ* fusion on the chromosome (Collier, 2000). Plasmid pBAC162 was linearized and used to transform strains ACN647, ACN649, and ACN651, replacing the wild-type *antA* gene with the *antA::lacZ* fusion on the chromosome. For both constructions, disruption of the *benA* or *antA* gene with the *lacZ* fusion abolished degradation of benzoate or anthranilate, respectively, preventing growth on benzoate or anthranilate. Therefore, strains were grown in LB plus muconate or benzoate as inducers. *lacZ* expression from the *benA* promoter was measured as  $\beta$ -galactosidase activity and reported as a percentage of the muconate-induced expression of control strains, which had either wild-type *benM* in the *ben-ant-ben* background (ACN862).

As reported previously, *benA* expression in strain ACN32 was inducible by both benzoate and muconate and *benA* expression was lost in strain ACN47, which lacked a functional BenM (Collier et al., 1998). The control strain, ACN862, also exhibited benzoate and muconate-inducible expression of *benA* (Figure 2.7). A strain lacking BenM in the *ben-ant-ben* background (ACN858) was also tested, and did not display *benA* expression in the presence of benzoate or muconate. The *benA* promoter expression in each of the *catB* promoter mutants was

induced by muconate, but not by benzoate (Figure 2.7). However, the strains only exhibited *benA* expression of approximately 30% of that observed for wild-type (Figure 2.7). This result is consistent with the findings from the *catB* structural gene mutants and also supports the proposed model of CatM-mediated expression of the *ben* genes in response to muconate. It is possible that expression is actually greater when muconate is generated internally as opposed to being provided exogenously as an inducer. Regardless, the level of expression is sufficient to allow growth on benzoate in the absence of BenM-mediated regulation.

Reporter strains containing *catB::lacZ* fusions were also constructed (Table 2.1). These reported strains were not able to grow on a carbon source that would permit intracellular generation of muconate. Because muconate was only available as an exogenous inducer and the uptake and transport of muconate into the cell is not well characterized, the catechol 1,2-dioxygenase and muconate cycloisomerase assays were considered more accurate assessments of gene expression.

### **Interaction between wild-type and mutant *catB* promoters and CatM**

Decreased affinity of CatM for the mutant *catB* promoters was considered a possible mechanism of decreasing expression of *catB* and subsequently CatB enzymatic activity. This physiological change may be responsible for increasing intracellular muconate and allowing expression of the *benA* promoter. Therefore, interactions between CatM and wild-type and mutant promoters were investigated. First, electrophoretic mobility shift assays were performed. Reactions combining wild-type or mutant promoter DNA with increasing concentrations of wild-type CatM were visualized using non-denaturing polyacrylamide gel electrophoresis. In these studies, 800 ng of CatM was sufficient to shift the entire band of wild-type *catB* promoter DNA (Figure 2.8, Lane

Wild-type #4). For the mutant containing an extra T in the site one spacer, some unbound DNA is still present with the addition of 800 ng of protein (Figure 2.8, Lane Extra T #4). This method was also used to examine the effect of point mutations in site 2 of the *catB* promoter and a similar result was observed. Qualitatively, this indicated that the affinity for the mutant promoter was diminished, but these assays did not allow calculation of binding constants.

Therefore, the affinity of interactions between the CatM regulatory protein and the *catB* promoter was also assessed using fluorescence anisotropy or fluorescence polarization. Synthetic oligonucleotides containing sites 1 and 2 of the *catB* promoter and a fluorescein label were combined with wild-type CatM and excited by a polarized light source. The affinity of CatM for the wild-type and mutant promoters was measured by the increase in polarization as DNA-protein complexes formed (Jameson, D. M. and J. C. Croney, 2003) (Figure 2.9).

When CatM was titrated into a binding reaction containing the wild-type *catB* promoter, polarization increased and a dissociation constant ( $K_d$ ) of 9 nM was calculated (Figure 2.10). When CatM was combined with the *catB* promoter containing an extra T between the half sites of site 1, a  $K_d$  of 43 nM was observed (Figure 2.11). Mutations in or near site 2 of the *catB* promoter also resulted in increased  $K_d$  of 39 nM and 22 nM, respectively (Figures 2.12, 2.13 and Table 2.4). Dissociation constants in this range are consistent with high affinity interactions (MacLean et al., 2008). The increased concentration of protein required to achieve half maximal DNA binding for the mutant promoters suggests that the affinity of CatM for these promoters is decreased relative to wild-type.

## DISCUSSION

Mutations in the *catB* promoter region were isolated based on their ability to restore growth on benzoate as a sole carbon source in the absence of a functional BenM regulatory protein. Mutations in *catB*, the gene encoding muconate cycloisomerase, were previously isolated and characterized. The investigation of the *catB* gene mutants lead to the hypothesis of a model of CatM-mediated expression of the *ben* genes described earlier in this chapter. The studies of the *catB* promoter mutants characterized in this study provide additional support for the model as well as additional information about DNA-protein interactions.

Although no significant difference in muconate concentration could be detected in the *catB* promoter mutants relative to wild-type, it cannot be concluded that muconate does not accumulate intracellularly. As described in this chapter, the *catB* promoter mutants have much longer lag phases and slower growth rates, making it difficult to compare the cultures at the same point during growth. Also, muconate concentration of 1 mM is toxic to cells (Gaines III et al., 1996). Therefore, it may not accumulate to a level that could be detected using HPLC. Finally, the relationship between intracellular and extracellular muconate concentration is unknown in *A. baylyi* so it is possible that the muconate measured in the culture supernatant does not accurately reflect the muconate concentration within the cells.

Similar to the *catB* gene mutants, *catB* promoter mutants exhibited an increased ratio of CatA to CatB specific activity. The enzyme activity data appears to support the proposed model of muconate-induced CatM-activated expression of the *ben* genes. The strains clearly exhibit increased CatA specific activity and decreased CatB activity compared to wild type. The imbalance of enzyme activity may result in an intracellular accumulation of muconate.

According to the model, CatA first converts catechol to muconate. As more muconate is produced, more CatM becomes effector bound and therefore active, which increases expression of the *catA* promoter and ensures that all available catechol will be converted to muconate. In the case of the original *catB* gene mutants, the less efficient CatB enzyme converted less muconate to muconolactone, presumably resulting in an intracellular accumulation of muconate. If the *catB* promoter mutations decrease expression of *catB*, they may create a similar effect by reducing the amount of CatB present in the cell, instead of by decreasing the efficiency of the enzyme. The discrepancy between *catA* and *catB* expression, and subsequently amount of active enzyme, results in optimal conversion of catechol to muconate, but reduced conversion of muconate to muconolactone, potentially allowing muconate to accumulate within the cell and ultimately reach a concentration sufficient to initiate CatM-activated expression of the *ben* genes.

Gene expression assays revealed that the *benA* promoter is being activated in the absence of BenM in the *catB* promoter mutants in response to muconate. Expression of the *benA* promoter at about 30% the level of wild-type was observed and this is consistent with previously characterized strains lacking BenM (Cospers et al., 2000). The relationship between intracellular and extracellular muconate is again an issue because cells respond differently when muconate is provided exogenously as opposed to generated intracellularly. Therefore, it may be that expression is actually higher in the *catB* promoter mutant strains than can be detected because of the reporter strain construction. The reporter strains contain a chromosomal *benA::lacZ* fusion and can no longer metabolize benzoate so the muconate must be added as an external inducer, which may not achieve optimal expression. The original *catB* gene mutants, were able to grow on anthranilate which does not require expression of the *ben* genes, but does lead to the

production of muconate. When grown under these conditions, these strains approached or exceeded wild-type levels of *benA* expression.

Finally, the fluorescence polarization experiments determined the affinity of CatM for the wild-type and mutant promoters. A lower  $K_d$  or lower concentration of protein required to achieve half-maximal DNA binding represents a greater affinity. The  $K_d$  for the wild-type and mutant promoters is not drastically different, but in this high affinity interaction the promoter mutations may reduce affinity enough to still allow *catB* expression at a level that permits growth, but not enough to rapidly convert muconate to muconolactone, increasing the intracellular concentration of muconate.

The combined results of longer lag phase and slower growth rates, increased CatA to CatB specific activity, increased expression of the *benA* promoter in the absence of BenM, and decreased affinity of CatM for the mutant *catB* promoters support a model of CatM-mediated regulation of the *ben* genes in response to increased intracellular muconate. According to this model, CatM has decreased affinity for the mutant *catB* promoters, resulting in more *catM* expression and less *catB* expression. The combined effect is more CatM present in the cell and more muconate available to activate the regulatory protein (Figure 2.14). In the absence of BenM, this combination may be capable of expressing the *benA* promoter enough to allow growth on benzoate as sole carbon source.

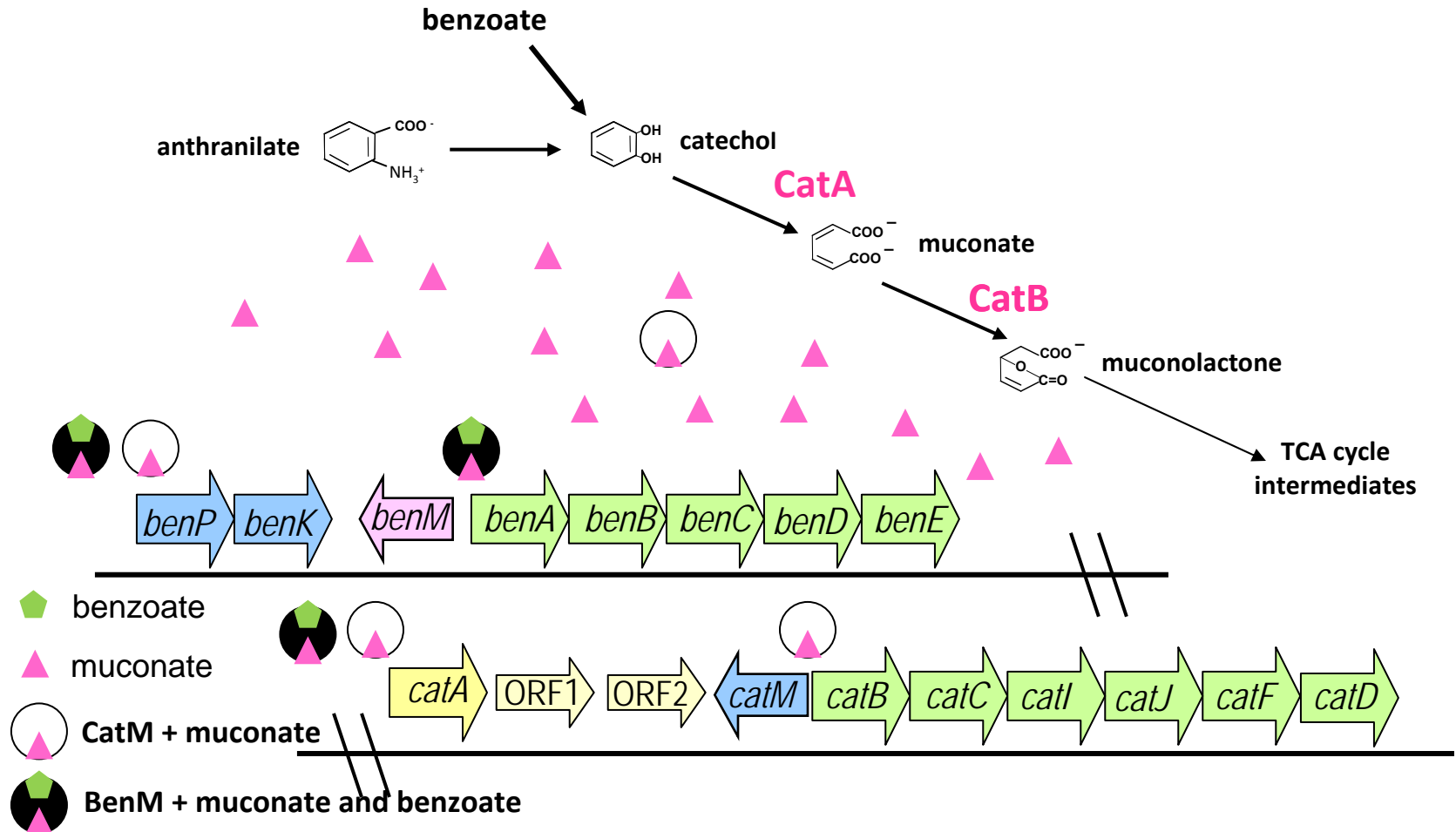


**Figure 2.1 Regulation of the *ben* and *cat* operons in wild-type cells.** The *ben* and *cat* genes are regulated by two homologous LTRs, *BenM* and *CatM*. Either regulator is sufficient for expression the *benP* and *catA* promoters, but only *BenM* can activate the *benA* promoter enough to allow growth on benzoate and only *CatM* can activate the *catB* promoter enough to allow rapid growth. Under normal conditions, *catA* and *catB* are expressed at about equal levels so that catechol is converted to muconate and the muconate is subsequently converted to muconolactone at approximately equal rates.

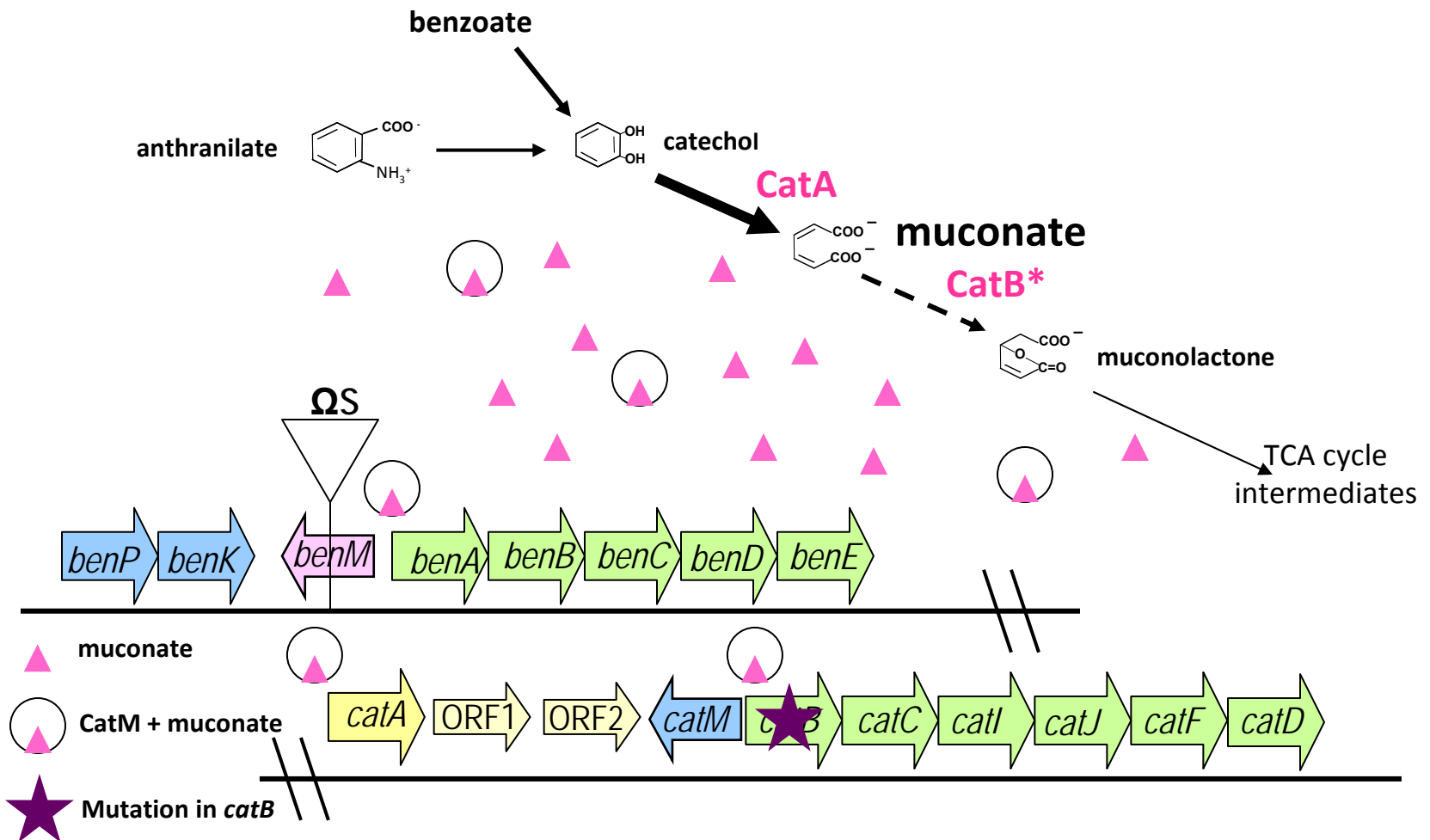


**Figure 2.2 Model of CatM-mediated expression of the *ben* genes.** In the absence of a functional BenM, mutations arise in *catB*, the gene encoding muconate cycloisomerase. The *catB* gene is still expressed normally and the substituted enzyme is still functional, but less efficient for converting muconate to muconolactone, (dashed arrow) causing muconate to accumulate. As this occurs, *catA* expression in response to muconate increases, (bold arrow) converting more catechol to muconate. Eventually enough intracellular muconate is present to allow CatM to activate the *ben* genes (Cosper et al., 2000).

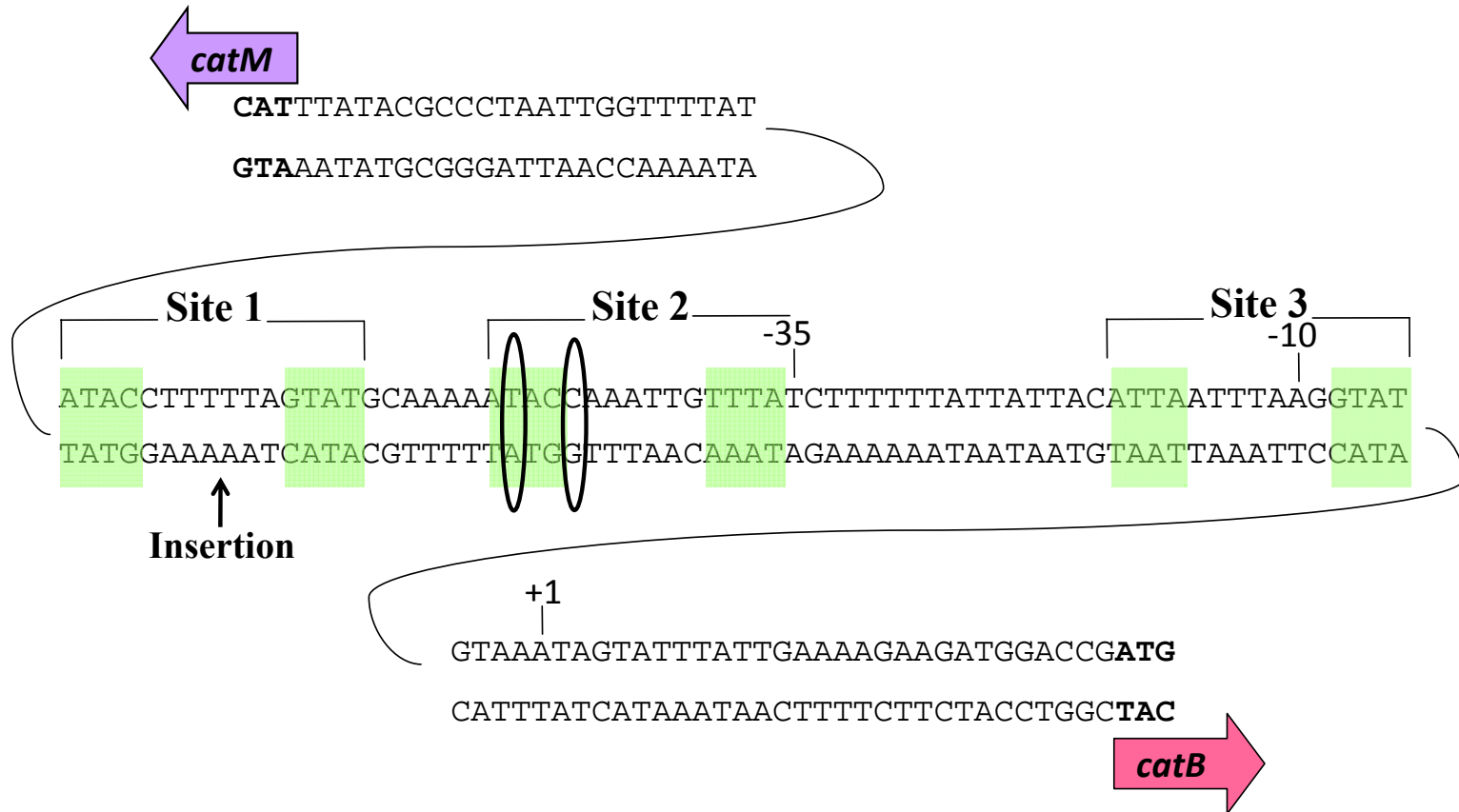


**Figure 2.3 Location of *catB* promoter mutations.** The insertion in the site one spacer was isolated three independent times (ACN150, ACN154, ACN651; allele # *catMB5150*). A T to C change in site two at -49 was isolated once (ACN649; allele # *catMB5649*). Point mutations at -46 were isolated three independent times: two C to T changes (ACN645, ACN647 allele # *catMB5645*), and one C to A change (ACN724; allele # *catMB5724*).

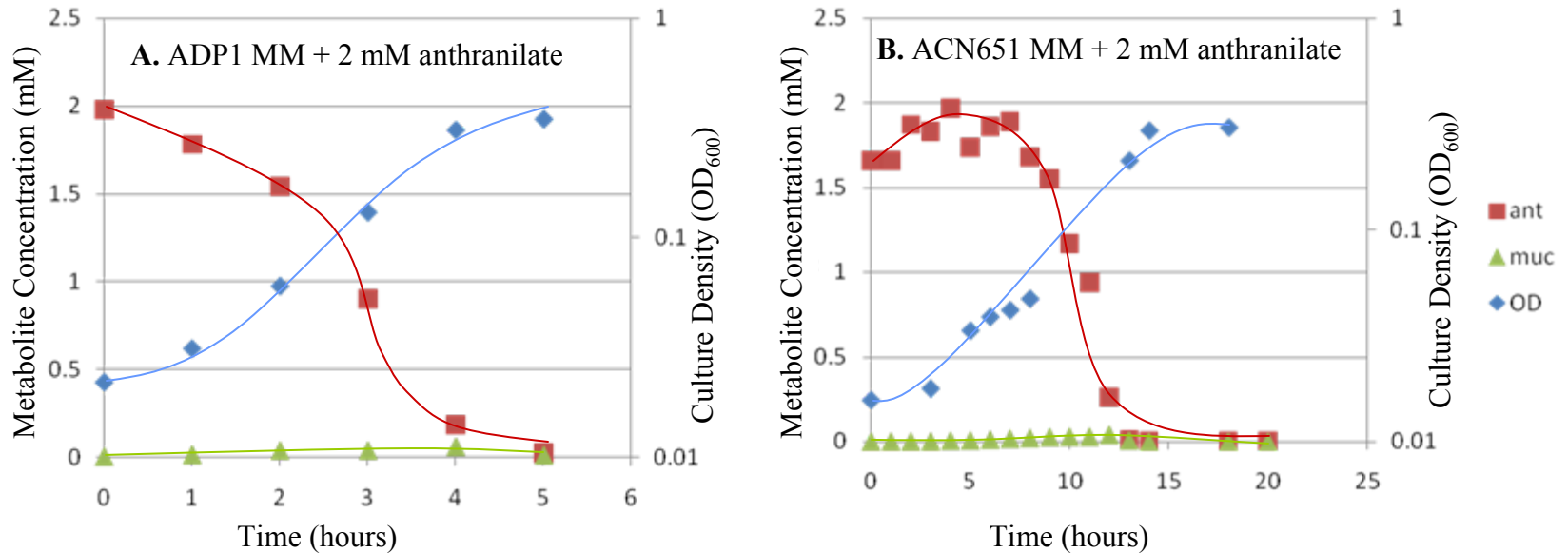


**Figure 2.4 Growth rate and metabolite concentration of wild-type and *catB* mutants.** Metabolite concentration is plotted on the left y-axis, muconate represented by green triangles and anthranilate represented by red squares. Culture density is represented on the right y-axis, represented by blue diamonds. Graph A shows a wild-type growth pattern in which cells begin consuming the anthranilate almost immediately, have a relative short lag phase, and double roughly every hour. Graph B represents the *catB* mutant with an extra T in site 1. This strain has a much longer lag phases and generation time.

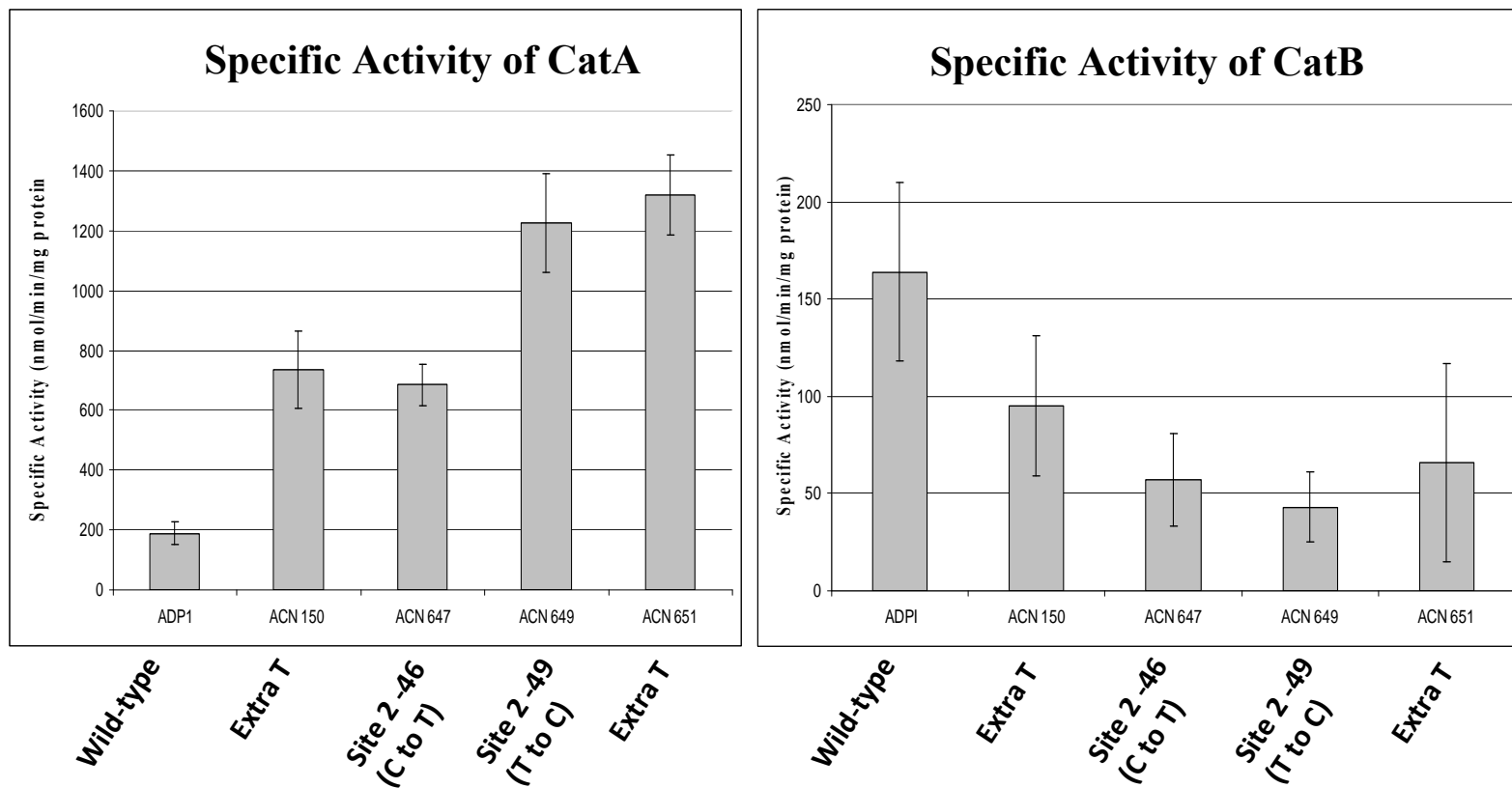


**Figure 2.5 Specific activity of CatA and CatB.** Specific Activity of CatA and CatB is defined as nmol of muconate produced/min/mg protein. The reported values are averages of at least three experiments.

## Ratio of CatA and CatB Activity

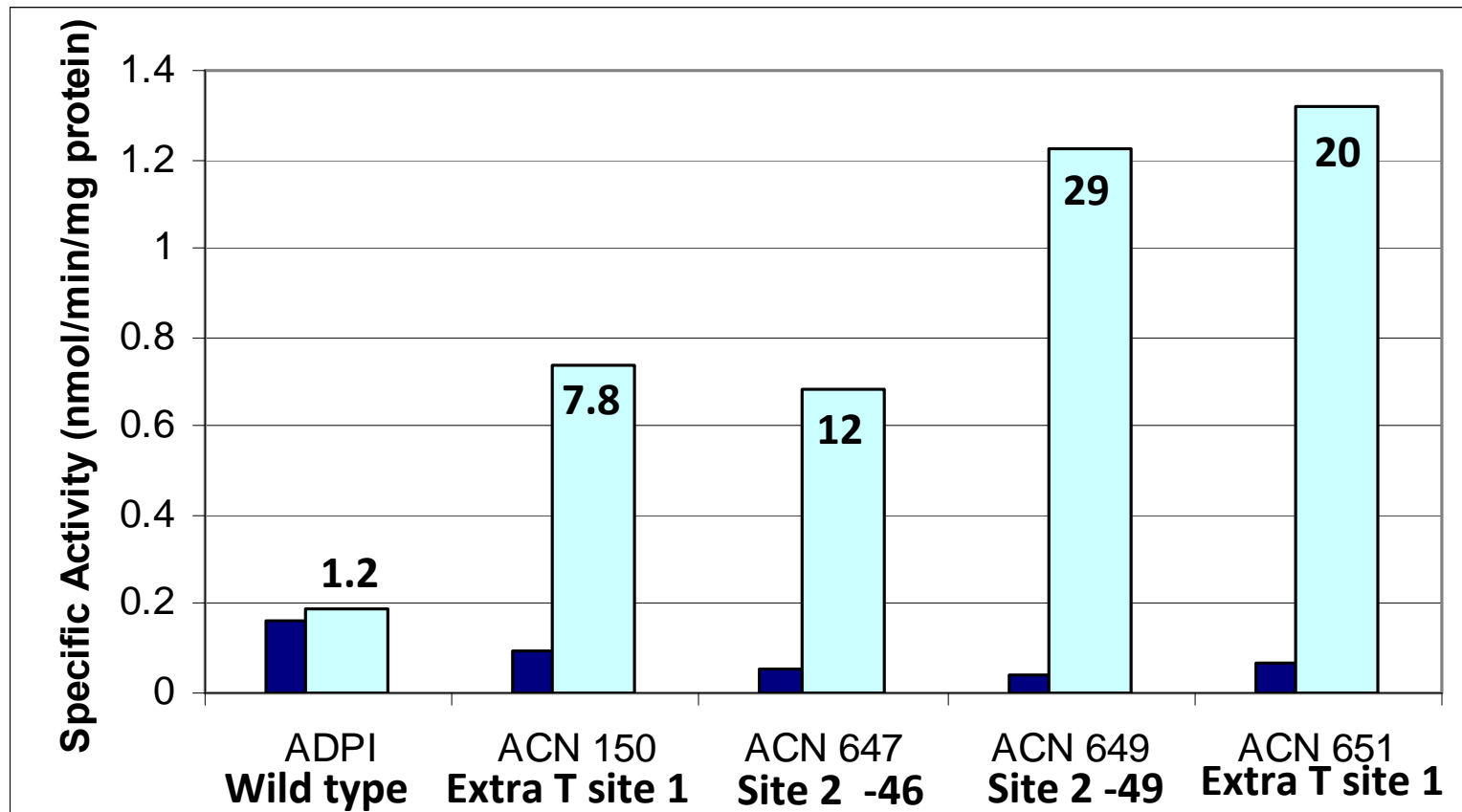


**Figure 2.6 Ratio of CatA to CatB activity.** The dark bars represent CatA activity and the open bars represent CatB activity. The ratio is equal to CatA activity divided by CatB activity and is shown at the top of the CatB activity bars.

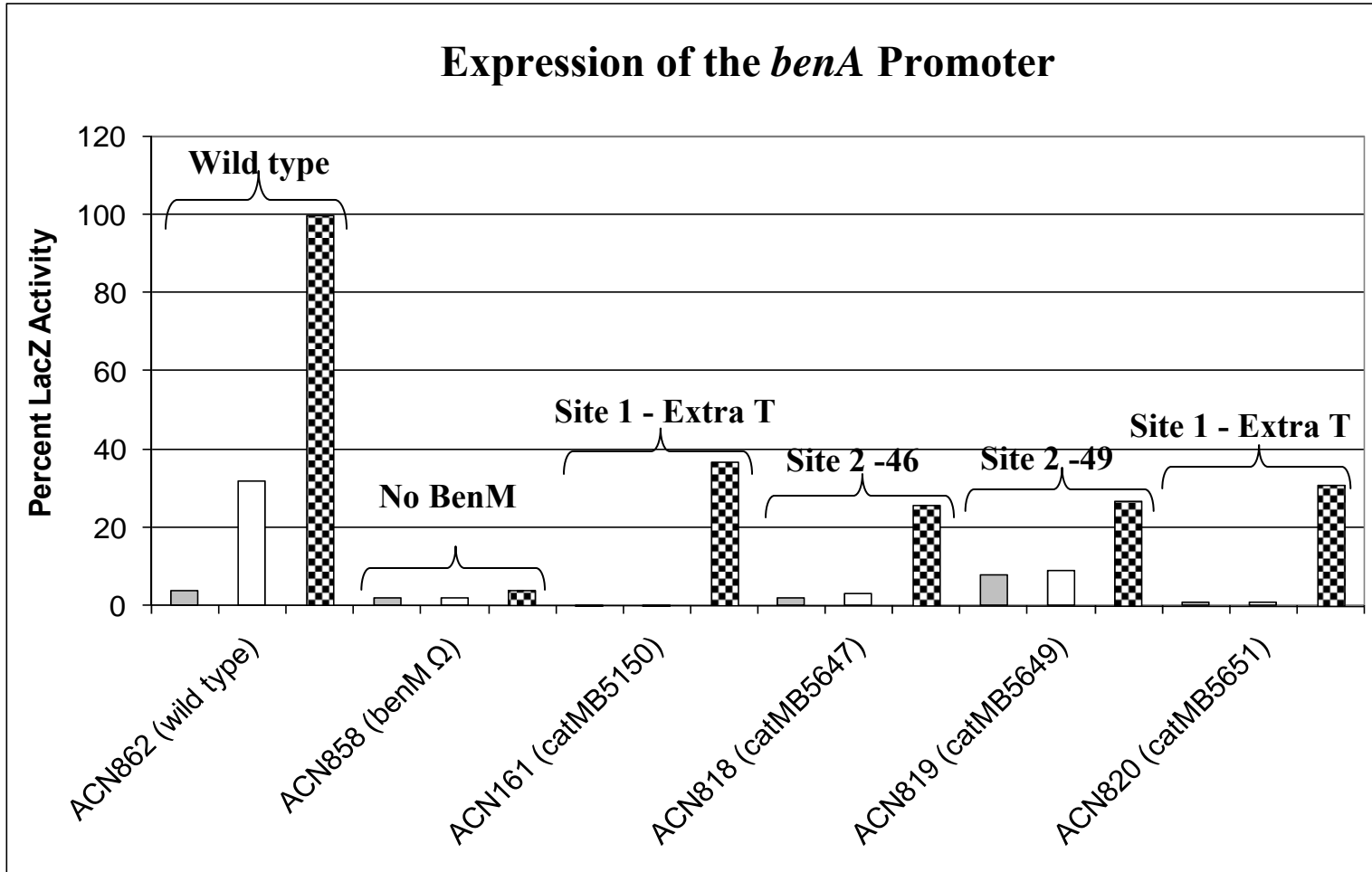


**Figure 2.7 *benA* expression in *catB* promoter mutants.**  $\beta$ -Galactosidase (LacZ) activity as a result of expression from a chromosomal *benA::lacZ* fusion. Values are reported as a percentage of the activity exhibited by an induced, wild type strain. Gray bars represent activity without inducer, white bars represent activity in response to benzoate, and checkered bars represent activity in response to muconate. The results shown are averages of at least three experiments.

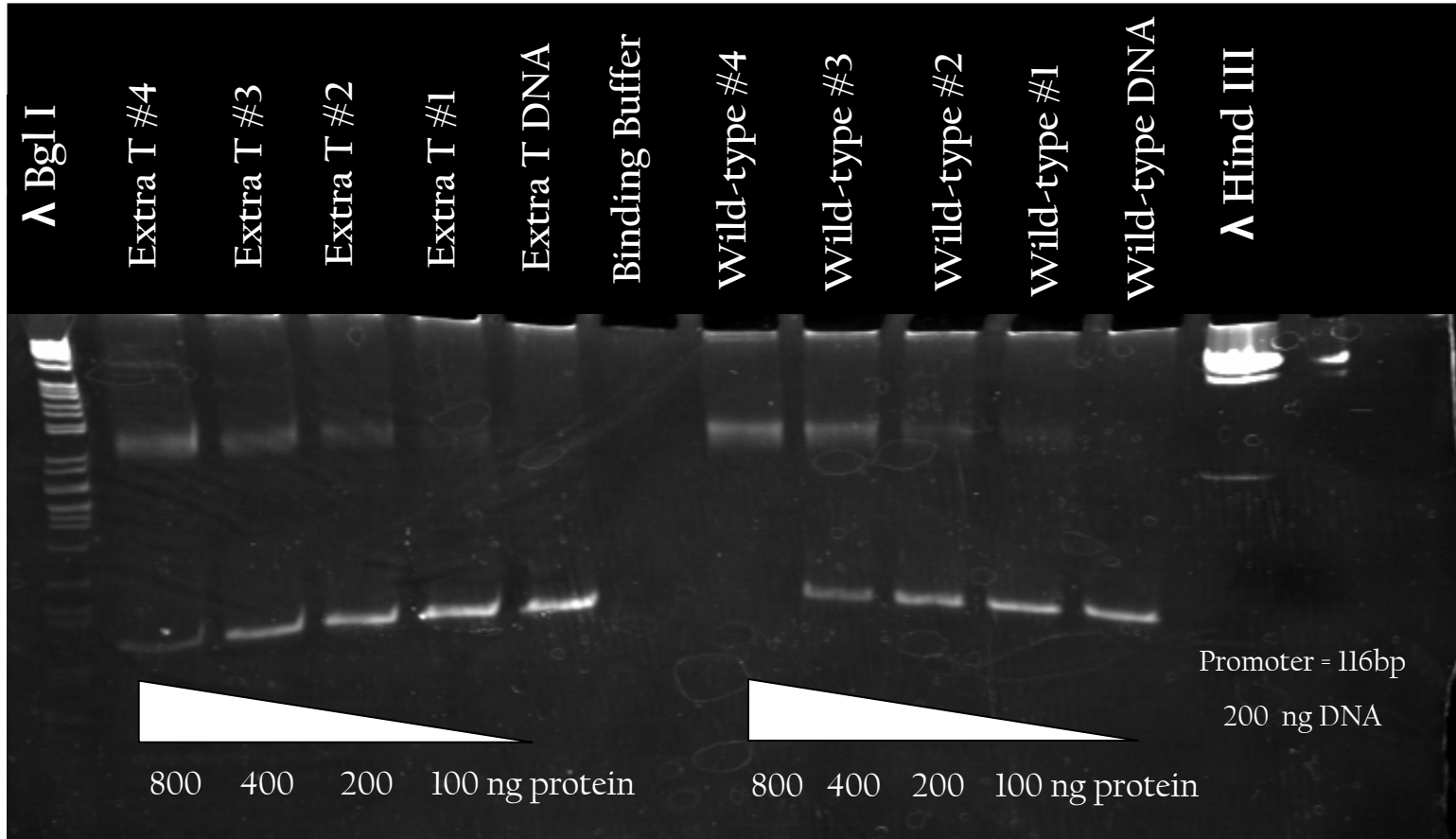


**Figure 2.8 EMSA of wild-type *catB* promoter and a *catB* promoter with an extra T in site one.** The lanes on the right show reactions between wild-type *catB* and wild-type CatM. As increasing amounts of protein are added, all DNA becomes associated with the protein. Reactions of mutant *catB* DNA and wild-type CatM are shown on the left. Even as protein concentration increases, some DNA remains unbound.

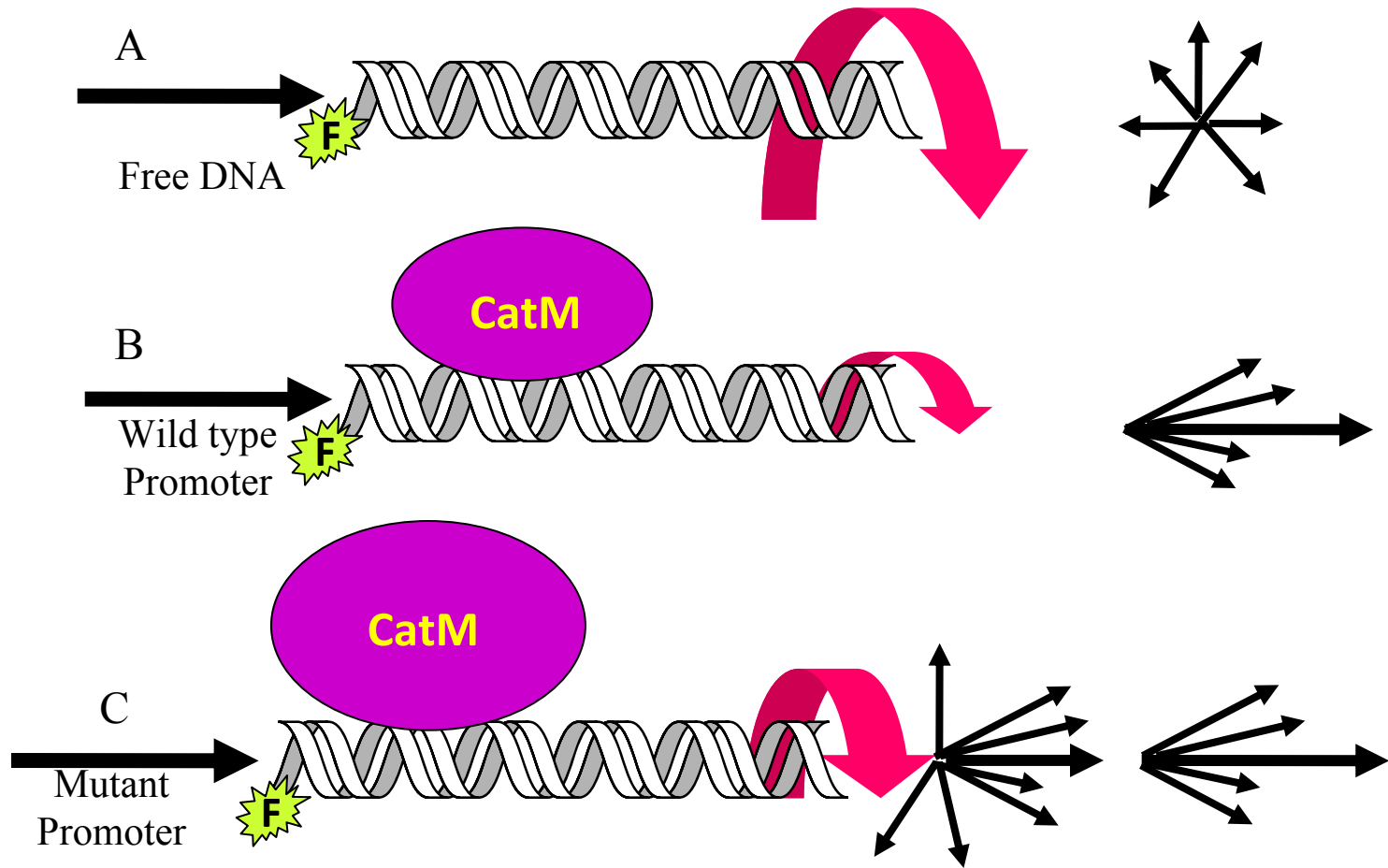


**Figure 2.9 Fluorescence Polarization Experiments.** A) Free DNA in solution it tumbles very rapidly as indicated by the large arrow. When excited by a polarized light source, the tumbling results in depolarization of the emitted light. B) If a protein that binds the DNA is added to the mixture, the tumbling will slow, indicated by smaller arrow, and the light will remain more polarized. C) If the protein does not have a high affinity for the DNA, then greater amounts of protein will be required to achieve polarization.

**A**

**Site 1**
**Site 2**

**F** - TTTATATACCTTTTTAGTATGCAAAAATACCAAATTGTTTATCTTT  
 AAATATATGGAAAAATCATACGTTTTTATGGTTTAACAAATAGAAA

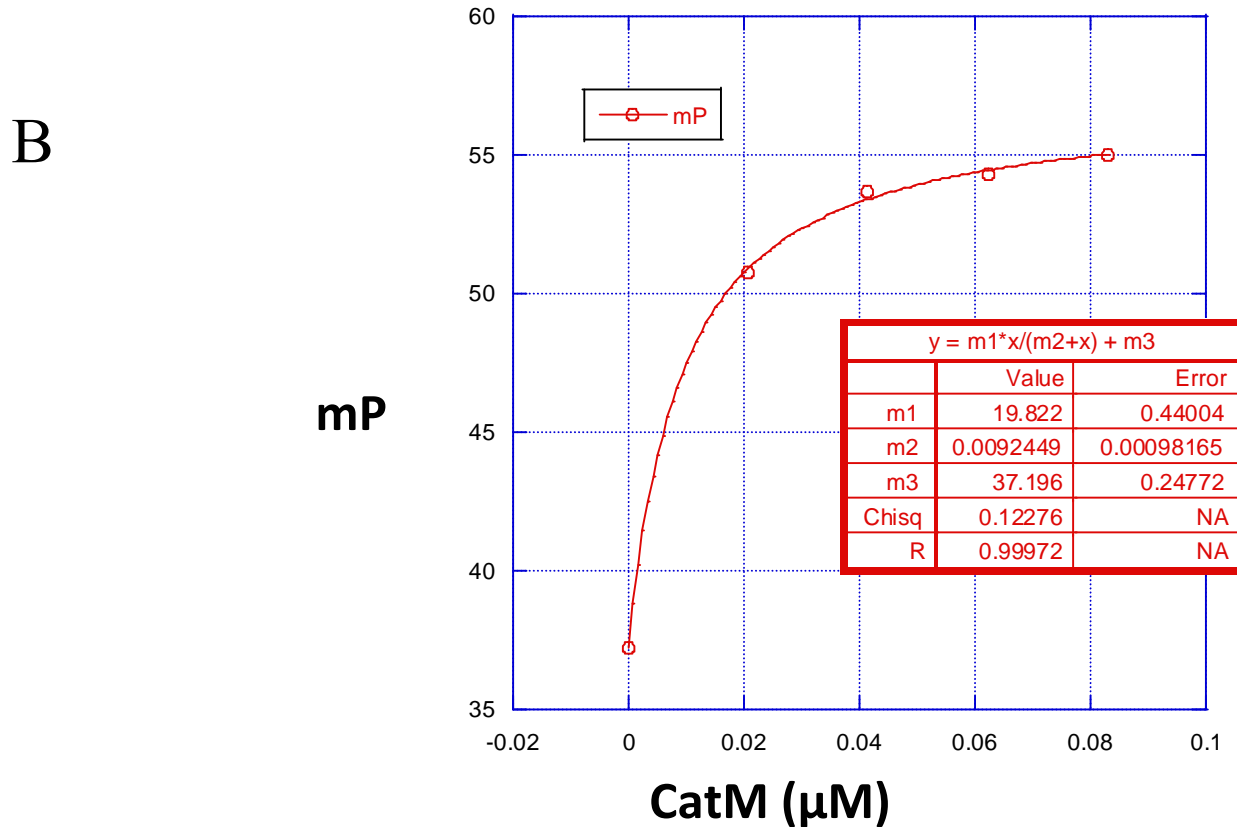


**Figure 2.10 Affinity of CatM for the wild-type *catB* promoter.** A) Wild-type *catB* promoter sequence. B) Representative binding curve of fluorescence polarization experiments. As CatM is added to the DNA solution, millipolarization increases, suggesting that CatM associates with the promoter. The dissociation constant ( $K_d$ ) is equal the concentration in nM of protein at which half-maximal DNA binding occurs. The m2 value calculated from the equation representing the best fit curve is equal to the  $K_d$ . For the wild-type promoter the  $K_d$  is  $7.4 \pm 1.6$  nM.

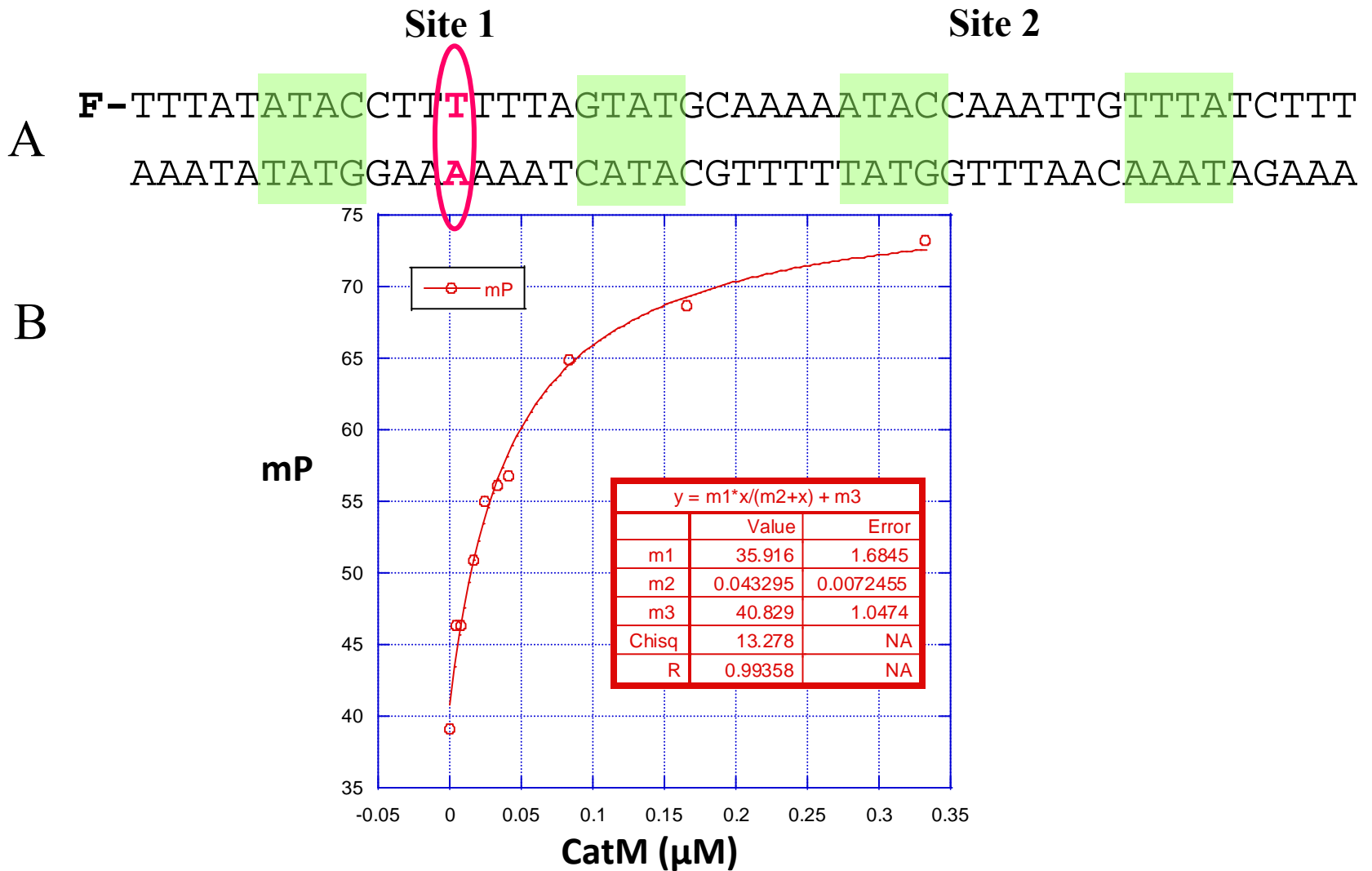


**Figure 2.11** Affinity of CatM for the *catB* promoter containing an extra T in the site 1 spacer. A) Mutant *catB* promoter sequence with inserted nucleotide circled. B) Representative binding curve of fluorescence polarization experiments. The  $K_d$  of this combination is  $70 \pm 24$  nM suggesting that CatM has decreased affinity for the mutant promoter because more protein is required for polarization.

**Site 1** **Site 2**

**F** - TTTATATACCTTTTTAGTATGCAAAAATACAAAATTGTTTATCTTT  
 A AAATATATGGAAAAATCATACGTTTTTATGTTTTAACAAATAGAAA

**B**

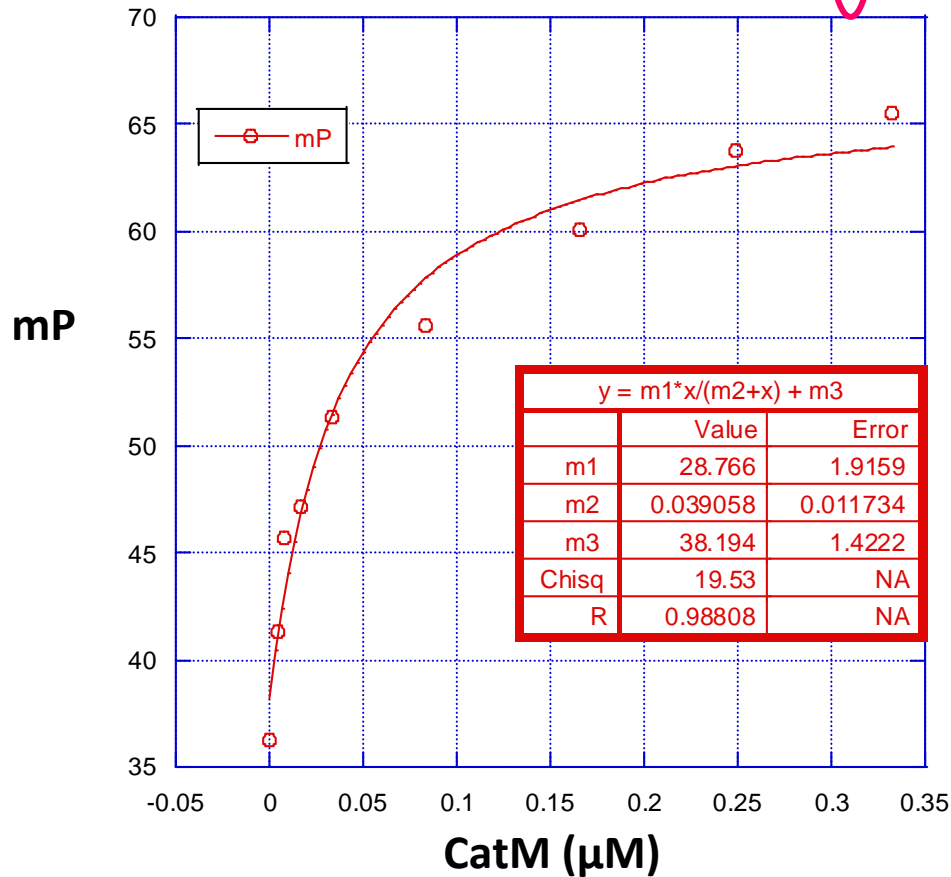


**Figure 2.12 Affinity of CatM for the *catB* promoter containing a C to T point mutation at -46.** A) Mutant *catB* promoter sequence. B) Representative binding curve of fluorescence polarization experiments. The  $K_d$  for this mutant is  $47 \pm 28$  nM again indicating decreased affinity for the promoter.

**Site 1** **Site 2**  
**F**-TTTATATACCTTTTTAGTATGCAAAAACACCAAATTGTTTATCTTT  
**A** AAATATATGGAAAATCATACGTTTTTGTGGTTTAACAAATAGAAA

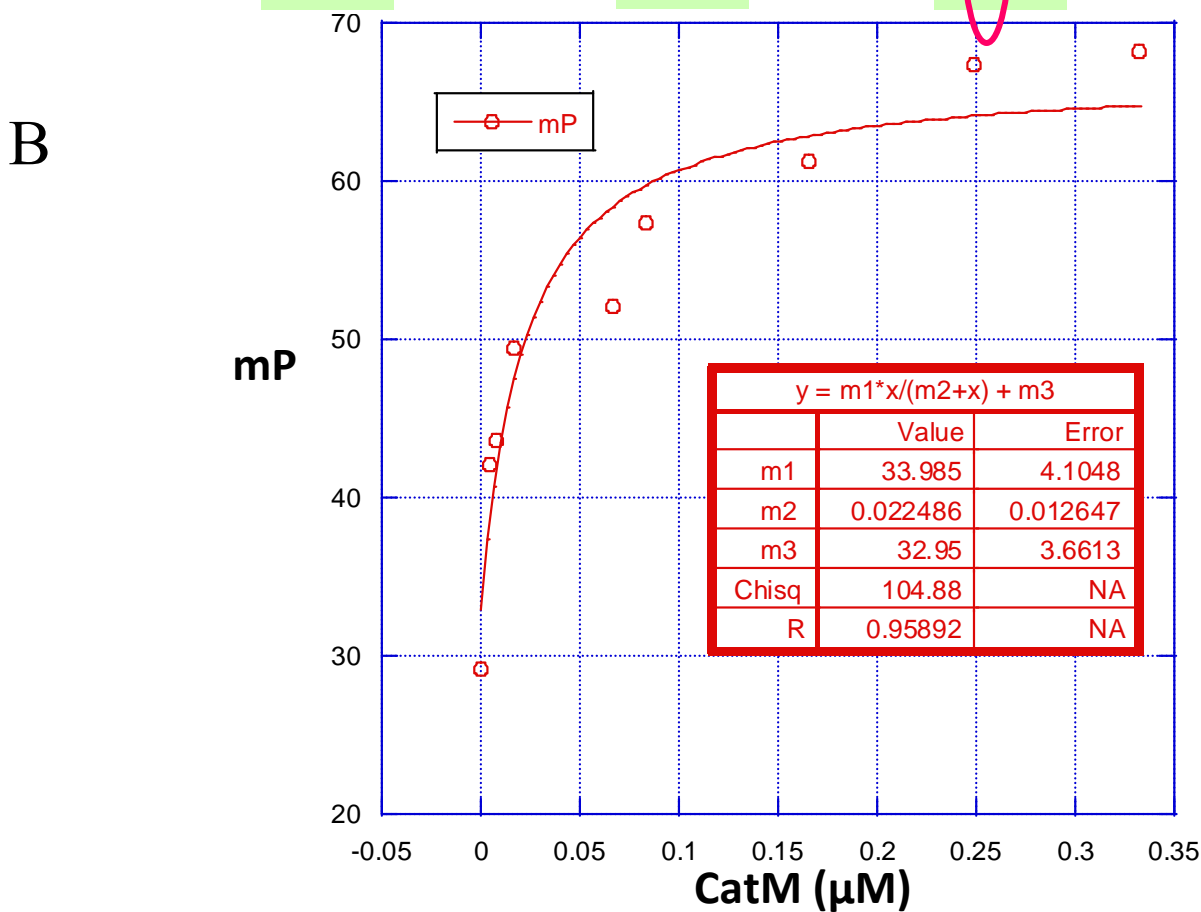


**Figure 2.13 Affinity of CatM for the *catB* promoter containing a T to C point mutation at -49.** A) Mutant *catB* promoter sequence. B) Representative binding curve of fluorescence anisotropy experiments. The  $K_d$  for this mutant is  $67 \pm 6$  nM, which suggests decreased affinity for this promoter.

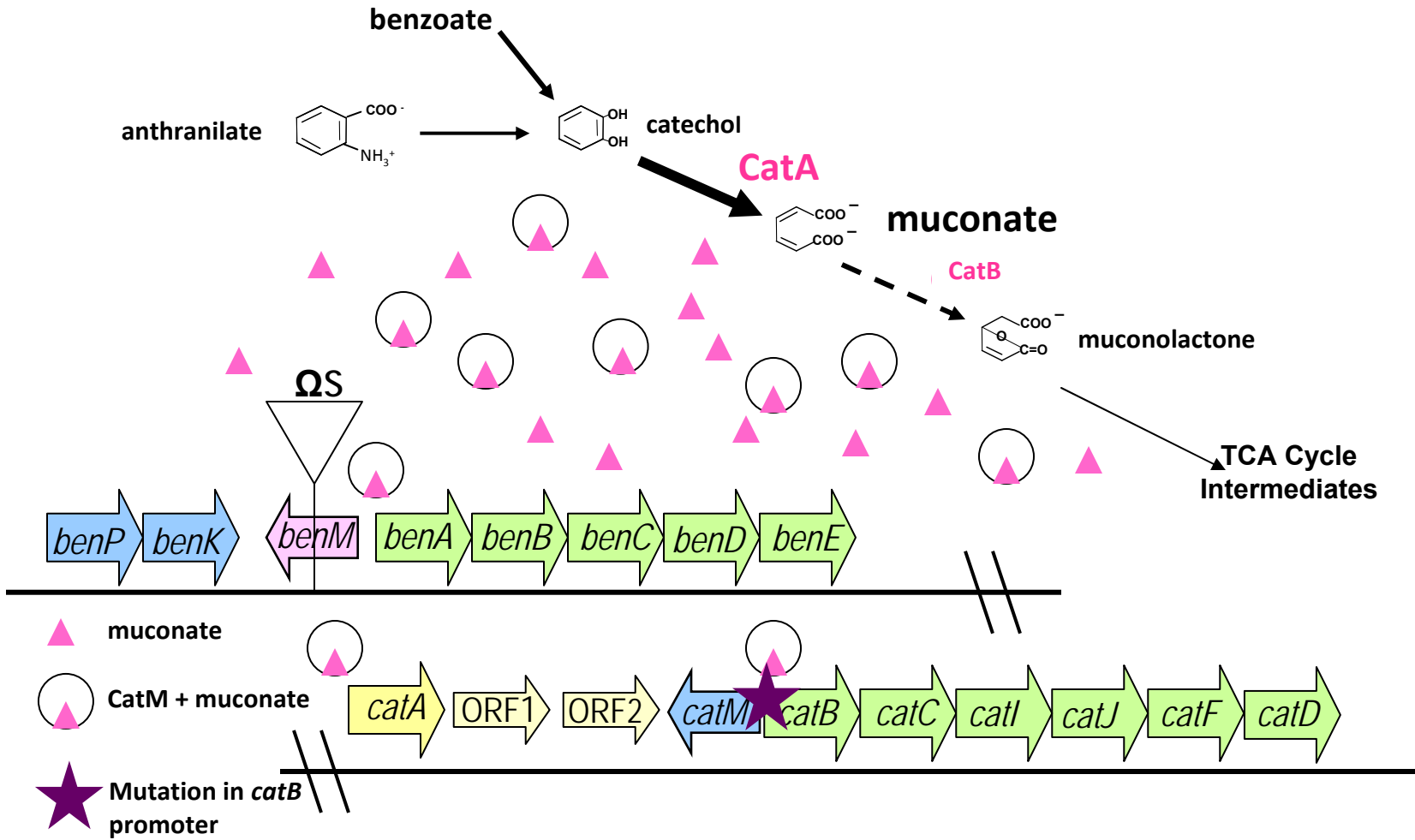


**Figure 2.14 Proposed model of CatM-mediated expression of the *benABCDE* operon.** In the absence of a functional BenM, mutations arise in the *catB* promoter. These mutations decrease the affinity of CatM for the promoter, resulting in increased *catM* expression as well as decreased *catB* expression. When less CatB enzyme is present, less muconate is converted to muconolactone, (dashed arrow) resulting in an increased concentration of intracellular muconate. The increased level of CatM can then become effector bound and active, increasing expression of *catA* and creating even more muconate from catechol (bold arrow) and ultimately activating transcription at *benA*.

**Table 2.1** Bacterial Strains and Plasmids

Strain or Plasmid	Relevant Characteristics	Reference
<i>A. baylyi</i> Strains		
ADP1	wild type	Juni E. and A. Janik, 1969
ISA36	<i>benM::</i> ΩS4036	Collier et al., 1998
ACN32	<i>benA::lacZ-Km<sup>r</sup>5032</i>	Collier et al., 1998
ACN47	<i>benM::</i> ΩS4036 <i>benA::lacZ-Km<sup>r</sup>5032</i>	Collier et al., 1998
ACN150	<i>benM::</i> ΩS4036 <i>catMB5150</i> [extra T between -62 and -66]	Collier, 2000
ACN154	<i>benM::</i> ΩS4036 <i>catMB5150</i>	Collier, 2000
ACN161	<i>benM::</i> ΩS4036 <i>benA::lacZ-Km<sup>r</sup>5032 catMB5150</i>	Collier, 2000
ACN616	Δ <i>antAB5616 antAB</i> replace <i>benAB5616</i> <sup>a</sup>	SH <sup>b</sup>
ACN617	Δ <i>antAB5616 ΔbenD5472 antAB</i> replace <i>benAB5616</i> <sup>a</sup>	SH <sup>b</sup>
ACN621	<i>benM::</i> ΩS4036 Δ <i>benD5472 ΔantAB5616 antAB</i> replace <i>benAB5616</i>	SH <sup>b</sup>
ACN858	<i>benM::</i> ΩS4036 Δ <i>benD5472 ΔantAB5616 antAB</i> replace <i>benAB5616 antA::lacZ-Kmr5032</i>	SH <sup>b</sup>
ACN859	<i>benM::</i> ΩS4036 Δ <i>benD5472 ΔantAB5616 antAB</i> replace <i>benAB5616 catB::lacZ-Kmr5032</i>	SH <sup>b</sup>
ACN645	<i>benM::</i> ΩS4036 Δ <i>antAB5616 antAB</i> replace <i>benAB5616 catMB5645</i> [C to T at -46]	SH <sup>b</sup>
ACN647	<i>benM::</i> ΩS4036 Δ <i>benD5472 ΔantAB5616 antAB</i> replace <i>benAB5616 catMB5645</i>	SH <sup>b</sup>
ACN649	<i>benM::</i> ΩS4036 Δ <i>benD5472 ΔantAB5616 antAB</i> replace <i>benAB5616 catMB5649</i> [T to C at -49]	SH <sup>b</sup>
ACN651	<i>benM::</i> ΩS4036 Δ <i>benD5472 ΔantAB5616 antAB</i> replace <i>benAB5616 catMB5151</i>	SH <sup>b</sup>
ACN652	<i>benM::</i> ΩS4036 Δ <i>benD5472 ΔantAB5616 antAB</i> replace <i>benAB5616 benMA5652</i> [T to C at -40]	SH <sup>b</sup>
ACN855	<i>benM::</i> ΩS4036 <i>catB::lacZ-Km<sup>r</sup>5032 catMB5150</i>	This study
ACN860	Δ <i>antAB5616 antAB</i> replace <i>benAB5616 antA::lacZ-Km<sup>r</sup>5032</i>	This study
ACN861	Δ <i>antAB5616 antAB</i> replace <i>benAB5616 catB::lacZ-Km<sup>r</sup>5032</i>	This study
ACN862	Δ <i>antAB5616 antAB</i> replace <i>benAB5616 ΔbenD antA::lacZ-Km<sup>r</sup>5032</i>	This study
ACN863	Δ <i>antAB5616 antAB</i> replace <i>benAB5616 ΔbenD catB::lacZ-Km<sup>r</sup>5032</i>	This study
ACN856	<i>benM::</i> ΩS4036 Δ <i>benD5472 ΔantAB5616 antAB</i> replace <i>benAB5616 antA::lacZ-Km<sup>r</sup>5032</i>	This study
ACN857	<i>benM::</i> ΩS4036 Δ <i>benD5472 ΔantAB5616 antAB</i> replace <i>benAB5616 catB::lacZ-Km<sup>r</sup>5033</i>	This study
ACN817	<i>benM::</i> ΩS4036 Δ <i>benD5472 ΔantAB5616 antAB</i> replace <i>benAB5616 antA::lacZ-Km<sup>r</sup>5032 catMB5645</i>	This study
ACN844	<i>benM::</i> ΩS4036 Δ <i>benD5472 ΔantAB5616 antAB</i> replace <i>benAB5616 catB::lacZ-Km<sup>r</sup>5032 catMB5645</i>	This study

ACN818	<i>benM::ΩS4036 ΔbenD5472 ΔantAB5616 antAB</i> replace <i>benAB5616 antA::lacZ-Km<sup>r</sup>5032 catMB5645</i>	This study
ACN845	<i>benM::ΩS4036 ΔbenD5472 ΔantAB5616 antAB</i> replace <i>benAB5616 catB::lacZ-Km<sup>r</sup>5032 catMB5645</i>	This study
ACN819	<i>benM::ΩS4036 ΔbenD5472 ΔantAB5616 antAB</i> replace <i>benAB5616 antA::lacZ-Km<sup>r</sup>5032 catMB5649</i>	This study
ACN846	<i>benM::ΩS4036 ΔbenD5472 ΔantAB5616 antAB</i> replace <i>benAB5616 catB::lacZ-Km<sup>r</sup>5032 catMB5649</i>	This study
ACN820	<i>benM::ΩS4036 ΔbenD5472 ΔantAB5616 antAB</i> replace <i>benAB5616 antA::lacZ-Km<sup>r</sup>5032catMB5651</i>	This study
ACN847	<i>benM::ΩS4036 ΔbenD5472 ΔantAB5616 antAB</i> replace <i>benAB5616 catB::lacZ-Km<sup>r</sup>5032catMB5651</i>	This study
ACN848	<i>benM::ΩS4036 ΔbenD5472 ΔantAB5616 antAB</i> replace <i>benAB5616 catB::lacZ-Km<sup>r</sup>5032 benMA5652</i>	This study
ACN849	<i>benM::ΩS4036 ΔbenD5472 ΔantAB5616 antAB</i> replace <i>benAB5616 antA::lacZ-Km<sup>r</sup>5032 benMA5652</i>	This study
Plasmids		
pUC19	Ap <sup>r</sup> ; cloning vector	Yanisch-Perron, C. et al., 1985
pKOK6	Source of promoterless <i>lacZ-Km<sup>r</sup></i> cassette	Kokotecz, W. and W. Lotz, 1989
pHP45	Ap <sup>r</sup> Sm <sup>r</sup> Sp <sup>r</sup> ; source of ΩS	Prentki, P. and Kirsch, H. M. 1984
pBAC14	<i>benM</i> in pRK415	Collier et al., 1998
pBAC54a	Ap <sup>r</sup> Km <sup>r</sup> ; <i>lacZ-Km<sup>r</sup></i> in NsiI site (3761) <sup>c</sup> in <i>benA</i> with adjacent <i>ben</i> region in pUC19	Collier, 2000
pBAC162	Ap <sup>r</sup> Km <sup>r</sup> ; <i>lacZ-Km<sup>r</sup></i> in NsiI site (2525) <sup>c</sup> of <i>antA</i> in pUC19 Ap <sup>r</sup>	Bundy et al., 1998
pBAC200	Tc <sup>r</sup> ; part of ORF1 and 2 - part of <i>catJ</i> and <i>catFD</i> , used to isolate the <i>catMB</i> region using the gap repair method	Cosper et al., 2000
pBAC238	Ap <sup>r</sup> ; wild-type <i>cat</i> region from ISA36	Cosper et al., 2000
pBAC675	Ap <sup>r</sup> Km <sup>r</sup> ; <i>lacZ-Km<sup>r</sup></i> in <i>catB</i> (13205-14225) <sup>c</sup> with <i>catJFD</i> (15660-17347) <sup>c</sup> in pUC19 Ap <sup>r</sup>	Ezezika et al., 2006
pBAC828	Ap <sup>r</sup> Km <sup>r</sup> ; wild type <i>catB</i> promoter <sup>d</sup> in pCR 2.1 topo cloning vector	this study
pBAC829	Ap <sup>r</sup> Km <sup>r</sup> ; mutant <i>catB</i> promoter containing <i>catMB5150</i> in pCR 2.1 topo cloning vector	this study
pBAC830	Ap <sup>r</sup> Km <sup>r</sup> ; mutant <i>catB</i> promoter containing <i>catMB5645</i> in pCR 2.1 topo cloning vector	this study
pBAC831	Ap <sup>r</sup> Km <sup>r</sup> ; mutant <i>catB</i> promoter containing <i>catMB5649</i> in pCR 2.1 topo cloning vector	this study

<sup>a</sup> *antAB* genes deleted from their native locus, *benAB* genes deleted, *antAB* replaced *benAB* on the chromosome and remain under control of *benA* promoter

<sup>b</sup> Mutations isolated and strains constructed by Sandra Haddad

<sup>c</sup> Position in the *ben-cat* sequence in GenBank entry (accession number AF009224)

<sup>d</sup> *catB* promoter from 1444593 to 1444709 genome sequence in GenBank entry (accession number NC005966.1)

**Table 2.2** - Sequences of *catB* promoters used during fluorescence polarization studies

Name	Sequence
ADP1 <i>catBS1S2</i>	F-TTTAT <u>ATAC</u> CTTTTTAGTATGCAAAAATACCAAATTGTTTATCTTT AAATATATGGAAAAATCATA <b>CG</b> TTTTTATGGTTTAACA <b>AA</b> TAGAAA
<i>catBS1S2</i> perfect	F-TTTAT <u>ATAC</u> CTTTTTAGTATGCAAAAATACCAAATTGGTATTCTTT AAATATATGGAAAAATCATA <b>CG</b> TTTTTATGGTTTAACCATAAGAAA
ACN150S1S2	F-TTTAT <u>ATAC</u> CTTTTTAGTATGCAAAAATACCAAATTGTTTATCTTT AAATATATGGAAAAATCATA <b>CG</b> TTTTTATGGTTTAACA <b>AA</b> TAGAA
ACN647S1S2	F-TTTAT <u>ATAC</u> CTTTTTAGTATGCAAAAATAC <b>AAA</b> ATTGTTTATCTTT AAATATATGGAAAAATCATA <b>CG</b> TTTTTATGTTTTTAACA <b>AA</b> TAGAAA
ACN649S1S2	F-TTTAT <u>ATAC</u> CTTTTTAGTATGCAAAAACACCAAATTGTTTATCTTT AAATATATGGAAAAATCATA <b>CG</b> TTTTT <b>GTG</b> GTTTAACA <b>AA</b> TAGAAA

F represents fluorescein label

Sites 1 and 2 are indicated by underlining

Mutations are indicated in bold

**Table 2.3** Summary of CatA and Cat B enzyme activity and generation times on anthranilate and succinate.

Strain	Relevant Characteristic(s)	Average sp act ( $\mu\text{mol}/\text{min}/\text{mg}$ of protein) <sup>a</sup> $\pm$ SD		CatA/CatB Ratio	Generation Time (min) <sup>b</sup> for growth on anthranilate	Generation Time (min) <sup>b</sup> for growth on succinate
		CatA	CatB			
ADP1	Wild type	0.189 $\pm$ 0.04	0.164 $\pm$ 0.05	1.2	55	57
ACN150	<i>benM::<math>\Omega</math>S4036 catMB5150</i>	0.888 $\pm$ 0.58	0.087 $\pm$ 0.06	10.2	99 <sup>c</sup>	55
ACN647	<i>benM::<math>\Omega</math>S4036 catMB5647</i>	0.685 $\pm$ 0.07	0.057 $\pm$ 0.02	12	78	44
ACN649	<i>benM::<math>\Omega</math>S4036 catMB5649</i>	1.23 $\pm$ 0.16	0.043 $\pm$ 0.02	28.6	144	57
ACN651	<i>benM::<math>\Omega</math>S4036 catMB5651</i>	1.32 $\pm$ 0.13	0.066 $\pm$ 0.05	20	174	49

<sup>a</sup> The values shown for CatA (catechol dioxygenase) and CatB (muconate cycloisomerase) are averages of at least three experiments.

<sup>b</sup> The values shown are averages of at least three experiments. The standard deviations were no more than 15% of the values shown.

<sup>c</sup> This strain was grown on benzoate instead of anthranilate.

**Table 2.4** Summary of protein-DNA dissociation constants determined by fluorescence anisotropy.

<b>Promoter Sequence</b>	<b>Dissociation Constant (nM)<sup>a</sup></b>
wild type <i>catB</i> promoter	7.4 ± 1.6
Extra T in site 2 of <i>catB</i> promoter	70 ± 24
Point mutation at -47 of <i>catB</i> promoter	47 ± 28
Point mutation at -50 of <i>catB</i> promoter	67 ± 6

<sup>a</sup> Reported values are an average of at least two experiments.

## CHAPTER III: CONCLUSIONS AND FUTURE DIRECTIONS

### Conclusions

The goal of this study was to increase understanding of the regulation of the genes involved in aromatic compound degradation, specifically the role of the LTTR, CatM, and the *catB* promoter region as well as the protein-DNA interactions controlling the *benABCDE* and *catBCIJFD* operons. Previously, more was known about BenM and the *benA* promoter region. Although there are similarities between the promoters and transcriptional regulators, differences in regulatory capability exist. Characterization of *catB* operator-promoter mutants provided more support for an existing model of CatM-mediated regulation of the *benA* promoter, and suggested that CatM and *catB* create another layer of intricacy in the regulatory scheme.

The results of these experiments demonstrated unique regulation of the *catB* region, and that alterations to this system could have distal regulatory effects, such as activation of the *benA* promoter. As described in chapter II, growth rate, metabolite concentration, gene expression, enzyme activity, and binding affinity data all indicate that the CatM regulatory protein is capable of activating transcription of the *benA* promoter in the presence of increased intracellular muconate. This highlights the presence of a complicated regulatory circuit governing the expression of a number of genes involved in aromatic compound degradation in which all enzymes and metabolites play critical roles.

## Future directions

In addition to generating data regarding the interactions between CatM and various promoters, the fluorescence polarization technique performed in this study provided a new method of examining the protein-DNA interactions controlling this system. The data generated during this study led to further development of this method in the lab. Current and future researchers may now be able to address additional questions of promoter specificity and alterations in affinity as a result of mutations. A series of mutants in the *benA* promoter with varying spacing between the ATAC-N<sub>7</sub>-GTAT LTTR consensus sequence has been constructed and the fluorescence polarization method would provide an excellent measure of affinity for these mutants (Bundy, unpublished data). This method could also be used to examine the current model of site 1, 2, and 3 of the promoters and their interactions with the regulatory proteins. Finally, this method could be used to investigate variant regulatory proteins to identify the key residues involved in DNA binding.

This work also contributed to the increasing knowledge of aromatic compound degradation and associated regulation, which may be critical for developing biotechnology. Confidence in predictable regulation of these pathways is crucial to the successful development of organisms capable of not only *in vitro* biosensing and bioremediation, but practical application as detectors of pollutants, pathogens, and explosive materials. In summary, the data acquired and proposed model of CatM-mediated *benA* expression contributed to a greater understanding of the regulation of aromatic compound degradation and the protein-DNA interactions involved, as well as provided some information that may lead to the development of necessary biotechnological products.

## REFERENCES

- Aravind, L., V. Anantharaman, S. Balaji, M. M. Babu, and L. M. Iyer.** 2005. The many faces of the helix-turn-helix domain: transcription regulation and beyond. *FEMS Microbiol Rev* **29**:231-62.
- Barbe, V., D. Vallenet, N. Fonknechten, A. Kreimeyer, S. Oztas, L. Labarre, S. Cruveiller, C. Robert, S. Duprat, P. Wincker, L. N. Ornston, J. Weissenbach, P. Marliere, G. N. Cohen, and C. Medigue.** 2004. Unique features revealed by the genome sequence of *Acinetobacter* sp. ADP1, a versatile and naturally transformation competent bacterium. *Nucleic Acids Res* **32**:5766-79.
- Bradford, M. M.** 1976. A rapid and sensitive method for the quantitation of microgram quantities of protein utilizing the principle of protein-dye binding. *Anal Biochem* **72**:428-54.
- Brennan, R. G.** 1993. The winged-helix DNA-binding motif: another helix-turn-helix takeoff. *Cell* **74**:773-6.
- Brzostowicz, P. C., A. B. Reams, T. J. Clark, and E. L. Neidle.** 2003. Transcriptional cross-regulation of the catechol and protocatechuate branches of the beta-ketoadipate pathway contributes to carbon source-dependent expression of the *Acinetobacter* sp. strain ADP1 *pobA* gene. *Appl Environ Microbiol* **69**:1598-606.
- Bundy, B. M.** 2001. Transcriptional Regulation of the *benABCDE* Operon of *Acinetobacter* Sp. Strain ADP1: BenM-Mediated Synergistic Induction in Response to the Inducer Compounds Benzoate and *Cis,Cis*-Muconate. The University of Georgia, Athens, GA.
- Bundy, B. M., A. L. Campbell, and E. L. Neidle.** 1998. Similarities between the *antABC*-encoded anthranilate dioxygenase and the *benABC*-encoded benzoate dioxygenase of *Acinetobacter* sp. strain ADP1. *J Bacteriol* **180**:4466-74.
- Bundy, B. M., L. S. Collier, T. R. Hoover, and E. L. Neidle.** 2002. Synergistic transcriptional activation by one regulatory protein in response to two metabolites. *Proc Natl Acad Sci U S A* **99**:7693-8.
- Cardinaux, J., J. C. Notis, Q. Zhang, N. Vo, J. C. Craig, D. Fass, R. G. Brennan, and R. H. Goodman.** 2000. Recruitment of CREB binding protein is sufficient for CREB-Mediated Gene Activation. *Molecular and Cellular Biology* **20**:1546-1552.
- Clark, T. J., C. Momany, and E. L. Neidle.** 2002. The *benPK* operon, proposed to play a role in transport, is part of a regulon for benzoate catabolism in *Acinetobacter* sp. strain ADP1. *Microbiology* **148**:1213-23.

- Cohen-Bazire, G. W. R. Sistrom, and R. Y. Stanier.** 1957. Kinetic studies of pigment synthesis by non-sulfur purple bacteria. *J. Cell. Comp. Physiol.* **49**:25-68.
- Collier, L. S.** 2000. Transcriptional regulation of benzoate degradation by BenM and CatM in *Acinetobacter* sp. Strain ADP1. The University of Georgia, Athens, GA. Ph.D. Thesis.
- Collier, L. S., G. L. Gaines III, and E. L. Neidle.** 1998. Regulation of benzoate degradation in *Acinetobacter* sp. strain ADP1 by BenM, a LysR-type transcriptional activator. *J Bacteriol* **180**:2493-501.
- Collier, L. S., N. N. Nichols, and E. L. Neidle.** 1997. *benK* encodes a hydrophobic permease-like protein involved in benzoate degradation by *Acinetobacter* sp. strain ADP1. *J Bacteriol* **179**:5943-6.
- Cosper, N. J., L. S. Collier, T. J. Clark, R. A. Scott, and E. L. Neidle.** 2000. Mutations in *catB*, the gene encoding muconate cycloisomerase, activate transcription of the distal *ben* genes and contribute to a complex regulatory circuit in *Acinetobacter* sp. strain ADP1. *J Bacteriol* **182**:7044-52.
- Craven, S. H., O. C. Ezezika, C. Momany, and E. Neidle.** 2008. LysR homologs in *Acinetobacter*: insights into a diverse and prevalent family of transcriptional regulators. In *Molecular Biology of Acinetobacter*, Gerischer, U. (ed.). Norfolk:Caister Academic Press, pp 163-202..
- Craven, S. H., O. C. Ezezika, S. Haddad, R. A. Hall, C. Momany, and E. Neidle.** 2009. Inducer responses of BenM, a LysR-type transcriptional regulator from *Acinetobacter baylyi* ADP1. *Molecular Microbiology* **72**: 881-894.
- Dagley, S.** 1986. Biochemistry of aromatic hydrocarbon degradation in *Pseudomonads*, p. 527-555. In J. R. Sokatch (ed.), *The Bacteria*. Academic Press, Inc., New York.
- Dagley, S.** 1978. Determinants of biodegradability. *Q Rev Biophys* **11**:577-602.
- de Berardinis, V., D. Vallenet, V. Castelli, M. Besnard, A. Pinet, C. Cruaud, S. Samair, C. Lechaplais, G. Gyapay, C. Richez, M. Durot, A. Kreimeyer, F. Le Fevre, V. Schachter, V. Pezo, V. Doring, C. Scarpelli, C. Medigue, G. N. Cohen, P. Marliere, M. Salanoubat, and J. Weissenbach.** 2008. A complete collection of single-gene deletion mutants of *Acinetobacter baylyi* ADP1. *Mol Syst Biol* **4**:174.
- Dmitrova, M., G. Younes-Cauet, P. Oertel-Buchheit, D. Porte, M. Schnarr, and M. Granger-Schnarr.** 1998. A new LexA-based genetic system for monitoring and analyzing protein heterodimerization in *Escherichia coli*. *Mol Gen Genet* **257**:205-12.
- Dove, S. L. and A. Hochschild.** 2005. How Transcription Initiation Can Be Regulated in Bacteria. In *The Bacterial Chromosome*. N. P. Higgins (ed), pp.

**Eby, D. M., Z. M. Beharry, E. D. Coulter, D. M. Kurtz, Jr., and E. L. Neidle.** 2001. Characterization and evolution of anthranilate 1,2 dioxygenase from *Acinetobacter* sp. Strain ADP1. *Journal of Bacteriology* **183**:109-118.

**Ezezika, O. C., L. S. Collier-Hyams, H. A. Dale, A. C. Burk, and E. L. Neidle.** 2006. CatM regulation of the *benABCDE* operon: functional divergence of two LysR-type paralogs in *Acinetobacter baylyi* ADP1. *Appl Environ Microbiol* **72**:1749-58.

**Ezezika, O. C., S. Haddad, T. J. Clark, E. L. Neidle, and C. Momany.** 2007. Distinct Effector Binding Sites Enable Synergistic Transcriptional Activation by BenM, a LysR-type Transcriptional Regulator. *Journal of Molecular Biology* **367**: 616-629.

**Ezezika, O. C., S. Haddad, E. L. Neidle, and C. Momany.** 2007. Oligomerization of BenM, a LysR-type transcriptional regulator: structural basis for the aggregation of proteins in this family. *Acta Crystallographica* **F63**: 361-368.

**Fewson, C. A.** 1991. The metabolism of aromatic compounds by *Acinetobacter*, p. 351-390. In *The Biology of Acinetobacter*, K. J. Towner, E. Borgogne-Berezin, and C.A. Fewson eds. (New York: Plenum Press), pp. 351-390.

**Gaines III, G. L., Smith, L., and E. L. Neidle.** 1996. Novel nuclear magnetic resonance spectroscopy methods demonstrate preferential carbon source utilization by *Acinetobacter calcoaceticus*. *J Bacteriol* **178**: 6833-6741.

**Gregg-Jolly, L. A., and L. N. Ornston.** 1990. Recovery of DNA from the *Acinetobacter calcoaceticus* chromosome by gap repair. *J Bacteriol* **172**:6169-72.

**Harwood, C. S., and R. E. Parales.** 1996. The beta-ketoadipate pathway and the biology of self-identity. *Annu Rev Microbiol* **50**:553-90.

**Huang, W. E., L. Huang, G. M. Preston, M. Naylor, J. P. Carr, Y. Li, A. C. Singer, A. S. Whiteley, H. Wang, W. E. Huang, H. Wang, H. Zheng, L. Huang, A. C. Singer, I. Thompson, and A. S. Whiteley.** 2006. Quantitative in situ assay of salicylic acid in tobacco leaves using a genetically modified biosensor strain of *Acinetobacter* sp. ADP1 Chromosomally located gene fusions constructed in *Acinetobacter* sp. ADP1 for the detection of salicylate. *Environ Microbiol* **7**:1339-48.

**Huang, W. E., H. Wang, H. Zheng, L. Huang, A. C. Singer, I. Thompson, and A. S. Whiteley.** 2005. Chromosomally located gene fusions constructed in *Acinetobacter* sp. ADP1 for the detection of salicylate. *Plant J* **46**:1073-83. *Environ Microbiol* **7**:1339-48.

**Huffman, J. L., and R. G. Brennan.** 2002. Prokaryotic transcription regulators: more than just the helix-turn-helix motif. *Curr Opin Struct Biol* **12**:98-106.

- Hütler, N. and W. Wackernagel.** 2008. Double illegitimate recombination events integrate DNA segments through two different mechanisms during natural transformation of *Acinetobacter baylyi*. *Mol Microbio* **67**: 984-995.
- Jameson, D. M., and J. C. Croney.** 2003. Fluorescence polarization: past, present and future. *Combinatorial Chemistry & High Throughput Screening* **6**:167-176.
- Jones, R. M., L. S. Collier, E. L. Neidle, P. A. Williams, R. M. Jones, V. Pagmantidis, and P. A. Williams.** 1999. *areABC* genes determine the catabolism of aryl esters in *Acinetobacter* sp. Strain ADP1. *J Bacteriol* **182**:2018-25.
- Jones, R. M., V. Pagmantidis, and P. A. Williams.** 2000. *sal* genes determining the catabolism of salicylate esters are part of a supraoperonic cluster of catabolic genes in *Acinetobacter* sp. strain ADP1. *J Bacteriol* genes determine the catabolism of aryl esters in *Acinetobacter* sp. Strain ADP1. *J Bacteriol* **181**:4568-75.
- Jourdan, A. D., and G. V. Stauffer.** 1998. Mutational analysis of the transcriptional regulator GcvA: amino acids important for activation, repression, and DNA binding. *J Bacteriol* **180**:4865-71.
- Juni, E.** 1978. Genetics and physiology of *Acinetobacter*. *Annu Rev Microbiol* **32**:349-71.
- Juni E., and A. Janik.** 1969. Transformation of *Acinetobacter calcoaceticus* (*Bacterium anitratum*). *Journal of Bacteriology* **98**: 281-288.
- Kok, R. G., D. A. D'Argenio, and L. N. Ornston.** 1998. Mutation analysis of PcbR and PcaU, closely related transcriptional activators in *Acinetobacter*. *J Bacteriol* **180**:5058-69.
- Kokotek, W., and W. Lotz.** 1989. Construction of a *lacZ*-kanamycin resistance gene cassette, useful for site-directed mutagenesis and as a promoter probe. *Gene* **84**: 467-471.
- Lalonde, S., D. W. Ehrhardt, D. Loque, J. Chen, S. Y. Rhee, and W. B. Frommer.** 2008. Molecular and cellular approaches for the detection of protein-protein interactions: latest techniques and current limitations. *Plant J* **53**:610-35.
- Lane, D., P. Prentki, and M. Chandler.** 1992. Use of gel retardation to analyze protein-nucleic acid interactions. *Microbiol Rev* **56**:509-28.
- Lochowska, A., R. Iwanicka-Nowicka, J. Zaim, M. Witkowska-Zimny, K. Bolewska, and M. M. Hryniewicz.** 2004. Identification of activating region (AR) of *Escherichia coli* LysR-type transcription factor CysB and CysB contact site on RNA polymerase alpha subunit at the *cysP* promoter. *Mol Microbiol* **53**:791-806.
- Lundblad, J. R., M. Laurance, and R. H. Goodman.** 1996. Fluorescence polarization analysis of protein-DNA and protein-protein interactions. *Mol Endocrinol* **10**:607-12.

- MacLean, A. M., M. I. Anstey, and T. M. Finan.** 2008. Binding site determinants for the LysR-type transcriptional regulator PcaQ in the legume endosymbiont *Sinorhizobium meliloti*. *J Bacteriol* **190**:1237-46.
- Meagher, R. B., K. L. Ngai, and L. N. Ornston.** 1990. Muconate Cycloisomerase. *Methods Enzymol.* **188**: 126-130.
- Muraoka, S., R. Okumura, N. Ogawa, T. Nonaka, K. Miyashita, and T. Senda.** 2003. Crystal structure of a full-length LysR-type transcriptional regulator, CbnR: unusual combination of two subunit forms and molecular bases for causing and changing DNA bend. *J Mol Biol* **328**:555-66.
- Neidle, E. L., C. Hartnett, S. Bonitz, and L. N. Ornston.** 1988. DNA sequence of the *Acinetobacter calcoaceticus* catechol 1,2-dioxygenase I structural gene *catA*: evidence for evolutionary divergence of intradiol dioxygenases by acquisition of DNA sequence repetitions. *J Bacteriol* **170**:4874-80.
- Neidle, E. L., and L. N. Ornston.** 1986. Cloning and expression of *Acinetobacter calcoaceticus* catechol 1,2-dioxygenase structural gene *catA* in *Escherichia coli*. *J Bacteriol* **168**:815-20.
- Ngai, K. L., E. L. Neidle, and L. N. Ornston.** 1990. Catechol and Chlorocatechol 1,2 dioxygenases. *Methods Enzym.* **188**: 122-126.
- Olsen, G. J., C. R. Woese, and R. Overbeek.** 1994. The winds of (evolutionary) change: breathing new life into microbiology. *J Bacteriol* **176**:1-6.
- Parsek, M. R., R. W. Ye, P. Pun, and A. M. Chakrabarty.** 1994. Critical nucleotides in the interaction of a LysR-type regulator with its target promoter region. *catBC* promoter activation by CatR. *J Biol Chem* **269**:11279-84.
- Prentki, P. and H. M. Kirsch.** 1984. In vitro insertional mutagenesis with a selectable DNA fragment. *Gene* **29**: 303-313.
- Rainey, F. A., E. Lang, and E. Stackebrandt.** 1994. The phylogenetic structure of the genus *Acinetobacter*. *FEMS Microbiol Lett* **124**:349-53.
- Reams, A. B. and E. L. Neidle.** 2004. Selection for gene clustering by tandem duplication. *Annu Rev Microbiol* **54**: 119-42.
- Romero-Arroyo, C. E., M. A. Schell, G. L. Gaines, 3rd, and E. L. Neidle.** 1995. *catM* encodes a LysR-type transcriptional activator regulating catechol degradation in *Acinetobacter calcoaceticus*. *J Bacteriol* **177**:5891-8.
- Schell, M. A.** 1993. Molecular biology of the LysR family of transcriptional regulators. *Annu Rev Microbiol* **47**:597-626.

**Segura, A., P. V. Bunz, D. A. D'Argenio, and L. N. Ornston.** 1999. Genetic analysis of a chromosomal region containing *vanA* and *vanB*, genes required for conversion of either ferulate or vanillate to protocatechuate in *Acinetobacter*. *J Bacteriol* **181**:3494-504.

**Shumacher, M. A., R. F. Pearson, T. Moller, P. Valentin-Hansen, and R. G. Brennan.** 2002. Structures of the pleiotropic translational regulator Hfq and an Hfq-RNA complex: a bacterial Sm-like protein. *EMBO* **21**:3546-3556.

**Stauffer, L. T., and G. V. Stauffer.** 2005. GcvA interacts with both the alpha and sigma subunits of RNA polymerase to activate the *Escherichia coli gcvB* gene and the *gcvTHP* operon. *FEMS Microbiol Lett* **242**:333-8.

**Towner, K. J., E. Borgogne-Berezin, and C. A. Fewson.** 1991. p. 1-24, *The Biology of Acinetobacter*. Plenum Press, New York.

**Tralau, T., J. Mampel, A. M. Cook, and J. Ruff.** 2003. Characterization of TsaR, an oxygen-sensitive LysR-type regulator for the degradation of p-toluenesulfonate in *Comamonas testosteroni* T-2. *Appl Environ Microbiol* **69**:2298-305.

**Vaneechoutte, M., D. M. Young, L. N. Ornston, T. De Baere, A. Nemeč, T. Van Der Reijden, E. Carr, I. Tjernberg, and L. Dijkshoorn.** 2006. Naturally transformable *Acinetobacter* sp. strain ADP1 belongs to the newly described species *Acinetobacter baylyi*. *Appl Environ Microbiol* **72**:932-6

**Yanisch-Perron, C., J. Vieira, and J. Messing.** 1985. Improved M13 Phage cloning vectors and host strains: nucleotide sequences of the M13mp18 and pUC19 vectors. *Gene* **33**:103-119.

**Young, D. M., D. Parke, and L. N. Ornston.** 2005. Opportunities for genetic investigation afforded by *Acinetobacter baylyi*, a nutritionally versatile bacterial species that is highly competent for natural transformation. *Annu Rev Microbiol* **59**:519-51.